Anharmonic Contributions to the Debye-Waller Factor*

GORDON A. WOLFE†‡
University of Missouri at Columbia, Columbia, Missouri 65201
AND
BERNARD GOODMAN
University of Cincinnati, Cincinnati, Ohio 45221
(Received 29 August 1968)

A method is presented for calculating anharmonic contributions to the Debye-Waller factor in the high-temperature limit in terms of direct-space sums. These sums are simpler quantities than those resulting from the phonon technique, in that there are no multiple integrals in reciprocal space and the frequencies and polarization vectors do not appear. They also have the advantage that no extreme assumptions about the form or range of the coupling parameters need be made. Calculations of anharmonic contributions to the Debye-Waller factor and the free energy are carried out for four models of copper. The values obtained for the mean-square displacement are compared with experimental values and with the calculations of others.

I. INTRODUCTION

THIS work is primarily concerned with the calculation of anharmonic contributions to the Debye-Waller factor for the scattering of x rays and neutrons by a crystal at temperatures T where quantum corrections are small. A number of calculations exist which are based on the small-amplitude or harmonic approximation.[1] Maradudin and Flinn[2] have given expressions for the anharmonic contributions in terms of multiple phonon integrations over the Brillouin zone. They made rough approximations to these formulas and estimated for lead a term in T^2 which is less than 10% of the harmonic term proportional to T for $T=2\Theta$, where Θ is the Debye temperature. They also estimated the T^3 terms, some of which are not isotropic, to be about 10^{-7} as large as the harmonic term. From the point of view of experiment a more accurate evaluation of the T^2 term is desirable, and also of the anistropic term which may be observable even when relatively small. The reason for its smallness is that the amplitude of thermal motion is small ($\sim$6% of the interatomic spacing; see Table IX) at Debye temperature, so that the crystalline directions of easy and hard motion are not very important. Nevertheless, the present work shows that the anisotropic part is considerably larger than the estimate above and might be seen.

The idea that motivated the present approach is that anharmonicity is chiefly a short-range effect due to ion repulsion in the lattice, so that a calculation using direct-space sums would be better suited than reciprocal-space integrations. It turns out that this is not true for all terms of interest and the procedure developed is a combination of reciprocal-space integration and direct-space summations. The situation is reminiscent of the Ewald methods[3] for lattice fields in which only long-range parts are calculated in reciprocal space. This procedure has several advantages over the complete reciprocal-space formulations.

First, there are no multiple integrals in reciprocal space and a *single* type of integral over the Brillouin zone must be done. This can be done quite accurately. The frequencies and polarization vectors do not appear, which also gives rise to considerable simplification.

Second, some of the analysis in Ref. 2 can only be done for a system in which the harmonic forces are also restricted to nearest-neighbor pairs, whereas experimental work indicates that one must consider, for example, interactions between at least third-nearest neighbors for copper[4] in order to describe the dispersion curves. For aluminum,[5] interactions between the origin atom and atoms in the eighth to fifteenth shells must be taken into account. In the present calculation inclusion of these additional interactions involves no additional complications.

Third, calculation of those anharmonic terms which are proportional to the fourth power of the scattering vector presents no problem in direct space, whereas Maradudin and Flinn were forced to approximations, whose effects are difficult to determine, in order to estimate them. It appears that a fortuitous large cancellation may have come in as a result of their approximations.

The use of direct-space sums was first proposed by Davies[6] for calculating anharmonic contributions to the free energy. The preceding remarks about the advantages of a combined reciprocal-space and direct-space summation procedure apply also to the free energy,

* Based in part on a Ph.D. dissertation submitted by G. A. W. to the University of Missouri in June 1967.
† NDEA Trainee and O. M. Stewart Fellow at the University of Missouri, Columbia.
‡ Present address: Southern Oregon College, Ashland, Ore. 97520.
[1] L. S. Salter, Advan. Phys. 14, 1 (1965).
[2] A. A. Maradudin and P. A. Flinn, Phys. Rev. 129, 2529 (1963).
[3] See, for example, C. Kittel, *Introduction to Solid State Physics*, (John Wiley & Sons, Inc., New York, 1956), 2nd ed., Appendix A.
[4] S. K. Sihna, Phys. Rev. 143, 422 (1966).
[5] J. L. Yarnell and J. L. Warren, in *Lattice Dynamics*, edited by R. F. Wallis (Pergamon Press, Inc., New York, 1965).
[6] R. O. Davies, *Fluctuation, Relaxation and Resonance in Magnetic Systems* (Oliver and Boyd, Edinburgh, 1961).

and we have included here a calculation of the third- and fourth-order anharmonicity contributions to the vibrational free energy of copper.

Section II collects the relevant theory. Starting from the cumulant expansion of the exponent of the Debye-Waller factor in powers of scattering vector, the perturbation expansion of each cumulant is developed along with a diagrammatic representation involving the harmonic pair-displacement correlation function. It is shown that only the "linked-cluster" subset of diagrams need be considered. Section III is devoted to the pair-displacement correlation function, its symmetry properties, and its relation to the dynamical matrix. Use of the pair-displacement function replaces the need to calculate phonon frequencies and polarizations and is computationally economical. The asymptotic behavior of the pair-displacement function at large separations is derived.

The particular sums needed in the third- and fourth-order anharmonic contributions to the Debye-Waller factor are enumerated in Sec. IV in terms of direct-space sums according to the rules given in Sec. II, and their convergence is studied. Section V develops briefly the expression for the thermal-expansion contribution to the Debye-Waller factor and Sec. VI does correspondingly for the anharmonic contribution to the Helmholtz free energy.

Numerical calculations are discussed in Sec. VII, which also contains tabulations of the results. Those include the harmonic pair-displacement correlation function, a comparison with its asymptotic expansion, and the various contributions to the Debye-Waller factor and to the vibrational free energy. The mean-square displacement, which dominates the Debye-Waller factor, is compared with experimental values and with other calculated values.

II. PERTURBATION EXPANSION

The Debye-Waller factor for atom l is the thermal average

$$e^{-M_l}\equiv\langle e^{i\kappa\cdot\mathbf{u}_l}\rangle=\mathrm{Tr}[e^{-\beta H}e^{i\kappa\cdot\mathbf{u}_l}]/\mathrm{Tr}e^{-\beta H}, \quad (2.1)$$

where H is the vibrational Hamiltonian, $\boldsymbol{\kappa}$ is the wave vector or scattering vector of the radiation involved, and $\mathbf{u}_l$ is the displacement of the atom from its reference position $\mathbf{R}_l$. This position will be assumed to be a center of inversion symmetry, so that the average of odd powers of $\mathbf{u}_l$ vanishes and (2.1) is a real quantity.

For harmonic vibrations the distribution function of the displacements is Gaussian. A convenient representation of nearly Gaussian distributions of a random variable X is by its cumulants or semi-invariants, which are defined in terms of its moment generating function $f(\alpha)$ as follows[7]:

$$f(\alpha)\equiv\langle e^{\alpha X}\rangle=\sum_{n=0}^{\infty}\frac{\alpha^n}{n!}\langle X^n\rangle\equiv\exp\left(\sum_{n=1}^{\infty}\frac{\alpha^n}{n!}\langle X^n\rangle_{\mathrm{cum}}\right)$$
$$=\exp\langle e^{\alpha X}-1\rangle_{\mathrm{cum}}. \quad (2.2)$$

The cumulants $\langle X^n\rangle_{\mathrm{cum}}$ can be expressed in terms of the moments $\langle X^m\rangle$ for $m\leq n$. The first four terms, which are all that are needed here, are

$$\begin{aligned}&\langle X\rangle_{\mathrm{cum}}=\langle X\rangle,\quad \langle X^2\rangle_{\mathrm{cum}}=\langle X^2\rangle-\langle X\rangle^2,\\ &\langle X^3\rangle_{\mathrm{cum}}=\langle X^3\rangle-3\langle X\rangle\langle X^2\rangle+2\langle X\rangle^3,\\ &\langle X^4\rangle_{\mathrm{cum}}=\langle X^4\rangle-4\langle X\rangle\langle X^3\rangle-3\langle X^2\rangle^2\\ &\qquad\qquad+12\langle X\rangle^2\langle X^2\rangle-6\langle X\rangle^4.\end{aligned} \quad (2.3)$$

For a Gaussian distribution $f(\alpha)$ is Gaussian, so that $\langle X\rangle_{\mathrm{cum}}$ and $\langle X^2\rangle_{\mathrm{cum}}$ are the only nonzero cumulants.

Applying (2.2) and (2.3) to (2.1) gives

$$\begin{aligned}\langle e^{i\kappa\cdot\mathbf{u}}\rangle&=\exp[-\tfrac{1}{2}\langle(\boldsymbol{\kappa}\cdot\mathbf{u})^2\rangle_{\mathrm{cum}}+(1/4!)\langle(\boldsymbol{\kappa}\cdot\mathbf{u})^4\rangle_{\mathrm{cum}}+\cdots]\\ &=\exp\{-\tfrac{1}{2}\langle(\boldsymbol{\kappa}\cdot\mathbf{u})^2\rangle+(1/4!)[\langle(\boldsymbol{\kappa}\cdot\mathbf{u})^4\rangle\\ &\qquad-3\langle(\boldsymbol{\kappa}\cdot\mathbf{u})^2\rangle^2]+\cdots\}.\end{aligned} \quad (2.4)$$

The thermal averages in (2.4) will be calculated by a perturbation expansion in $H-H_0$, where H_0 is the harmonic Hamiltonian defined by retaining only up to the quadratic terms in the Taylor expansion of the configurational potential energy V in powers of the displacements. Thus

$$\langle\mathcal{O}\rangle=\mathrm{Tr}[e^{-\beta H_0}U(\beta)\mathcal{O}]/\mathrm{Tr}[e^{-\beta H_0}U(\beta)] \quad (2.5)$$
$$=\langle U(\beta)\mathcal{O}\rangle^0/\langle U(\beta)\rangle^0, \quad (2.6)$$

where

$$U(\beta)=e^{\beta H_0}e^{-\beta H}, \quad (2.7)$$

and the superscript zero denotes the thermal average for a system with the Hamiltonian H_0. In order to calculate the Debye-Waller factor to order κ^4 in the exponent, we need the following terms:

$$\langle(\boldsymbol{\kappa}\cdot\mathbf{u}_0)^n\rangle=\langle U(\beta)(\boldsymbol{\kappa}\cdot\mathbf{u}_0)^n\rangle^0/\langle U(\beta)\rangle^0, \quad (2.8)$$

for $n=2$ and 4. It will be seen later in this section [Eq. (2.23)] that the linked-cluster expansion gives directly the cumulants in the first line of (2.4) rather than the individual averages on the second line.

We consider a Bravais lattice

$$\mathbf{R}_l=l_1\mathbf{a}_1+l_2\mathbf{a}_2+l_3\mathbf{a}_3, \quad (2.9)$$

about which the configuration potential energy is expanded in a Taylor's series in the displacement components $u_l{}^\alpha$,

$$V(\mathbf{r}_1,\mathbf{r}_2,\cdots)=\sum_{j=0}^{\infty}V_j, \quad (2.10)$$

[7] M. G. Kendall and A. Stewart, *The Advanced Theory of Statistics* (Charles Griffen and Co., Ltd., London, 1958), Chap. 3.

where

$$V_j=(j!)^{-1}\sum_{\substack{\alpha_1\alpha_2\cdots\alpha_j\\ l_1l_2\cdots l_j}} V_{l_1\cdots l_j}{}^{\alpha_1\cdots\alpha_j}u_{l_1}{}^{\alpha_1}\cdots u_{l_j}{}^{\alpha_j} \quad (2.11)$$

and

$$V_{l_1\cdots l_j}{}^{\alpha_1\cdots\alpha_j}=\frac{\partial^j V(\mathbf{R}_1,\mathbf{R}_2,\cdots)}{\partial R_{l_1}{}^{\alpha_1}\cdots\partial R_{l_j}{}^{\alpha_j}} \quad (2.12)$$

are the coupling parameters (CP) of jth order.

Invariance of the potential energy under rotations and translations (both infinitesimal and those of the discrete symmetries of the lattice) leads to relations between the CP.[8] The ones useful to us are listed here. First, the CP are unchanged when any vertical pair of indices is interchanged with any other pair. Invariance under infinitesimal translation of all the atoms leads to

$$\sum_{l_j} V_{l_1\cdots l_j}{}^{\alpha_1\cdots\alpha_j}=0. \quad (2.13a)$$

Invariance under lattice translations gives

$$V_{l_1l_2\cdots l_{j-1}l_j}{}^{\alpha_1\alpha_2\cdots\alpha_{j-1}\alpha_j}=V_{l_1'l_2'\cdots l_{j-1}'0}{}^{\alpha_1\alpha_2\cdots\alpha_{j-1}\alpha_j}, \quad (2.13b)$$

with $\mathbf{l}_i'=\mathbf{l}_i-\mathbf{l}_j$, $i=1, 2, \cdots, j-1$. Finally, if $\mathcal{T}$ is a discrete symmetry rotation with matrix $\mathbf{T}$ such that $\mathcal{T}\mathbf{R}_l=\mathbf{R}_{l'}$, then, using the summation convention,

$$V_{l_1'l_2'\cdots l_j'}{}^{\alpha_1'\alpha_2'\cdots\alpha_j'}=T_{\alpha_1'\alpha_1}T_{\alpha_2'\alpha_2}\cdots T_{\alpha_j'\alpha_j}V_{l_1l_2\cdots l_j}{}^{\alpha_1\alpha_2\cdots\alpha_j}. \quad (2.13c)$$

The Hamiltonian is written

$$H=H_0+V_A, \quad (2.14)$$

where

$$H_0\equiv\sum_l\frac{\mathbf{P}_l^2}{2M}+V_0+V_2 \quad (2.15)$$

is the Hamiltonian for a harmonic crystal and

$$V_A\equiv\sum_{j=3}^{\infty}V_j \quad (2.16)$$

is the anharmonic part of H, which is treated as a perturbation. Linear terms V_1 would exist only for atoms at the surface when there is an applied stress.

Perturbation Expansion in Terms of Harmonic Pair-Displacement Correlations (Wick Theorem)

Since anharmonic effects are significant mainly at higher temperatures in the systems of interest to us here, we shall consider them classically first. Quantum effects will be considered later. Then

$$U(\beta)=e^{-\beta V_A}. \quad (2.17)$$

The kth term in the expansion in powers of V_A of the numerator of (2.8) for, say $n=2$, is a sum over $j(1)$, $j(2)$, $\cdots$, $j(k)$ of

$$\frac{(-\beta)^k}{k!}\frac{\sum_{\alpha\beta}\kappa_\alpha\kappa_\beta}{j(1)!\cdots j(k)!}\sum_{J_{11}\cdots J_{kj(k)}}V_{J_{11}\cdots J_{1j(1)}}\cdots V_{J_{k1}\cdots J_{kj(k)}}\times\langle u_{J_{11}}u_{J_{12}}\cdots u_{J_{kj(k)}}u_0{}^\alpha u_0{}^\beta\rangle^0. \quad (2.18)$$

Each J stands for an index pair

$$\binom{\alpha}{l}$$

and j is the order of the CP involved.

The harmonic thermal averages of products of displacements in (2.18) can be written as the sum of products of harmonic pair correlations.[6] For n even,

$$\langle u_{J_1}u_{J_2}\cdots u_{J_n}\rangle^0=\sum_{\text{All pairings}}\langle u_{J_1}u_{J_j}\rangle^0\cdots\langle u_{J_k}u_{J_l}\rangle^0, \quad (2.19)$$

the sum being over all partitions of $J_1,\cdots, J_n$ into $\frac{1}{2}n$ pairs, order being immaterial. For n odd, the average on the left side of (2.19) vanishes. Equation (2.19) is the analog of the Wick theorem in many-body theory[9] and leads similarly to a diagram representation of the perturbation series. The distribution function $\rho^0(\mathbf{u}_1,\mathbf{u}_2,\cdots)$ is proportional to $\exp[-\beta V_2(\mathbf{u}_1,\mathbf{u}_2,\cdots)]$ and defines a multivariate Gaussian distribution. Relations (2.19) is a familiar property of such distributions which antedates the Wick theorem for fermions and bosons by many years.

When (2.19) is inserted into (2.18), each summand can be represented in terms of the following elements: (a) a pair correlation $\langle u_pu_q\rangle^0$ by a line connecting the points p and q; (b) a CP factor $-\beta V_{J_1\cdots J_1}$ by a vertex of order j containing the points $J_1,\cdots, J_j$ (for simplicity the vertex with its points will be shown as a heavy dot; a line which connects two points of the same vertex will appear as a bubble); and (c) the points

$$I_1=\binom{\alpha}{0},\quad I_2=\binom{\beta}{0}$$

and the associated factors κ_α and κ_β by a κ-vertex, denoted by a cross. Higher-order κ vertices [of order n in (2.8)] will be needed and will also be denoted by a cross. This prescription defines a *labeled* diagram. As an example, consider the diagram in Fig. 1(a). Since the points comprising a vertex are not shown, the *same* labeled diagram might be represented in apparently different ways. For example, Figs. 1(a) and 1(b) are the same. The contribution associated with this labeled diagram is defined as the sum over all numerical values of

[8] G. Leibfried and W. Ludwig, *Solid State Physics*, edited by F. Seitz and D. Turnbull (Academic Press Inc., New York, 1961), Vol. 12, pp. 283–288.

[9] A. A. Abrikosov, L. P. Gorkov, and I. E. Dzyaloshinski, *Methods of Quantum Field Theory in Statistical Physics* (Prentice-Hall, Inc., Englewood Cliffs, N. J., 1963).

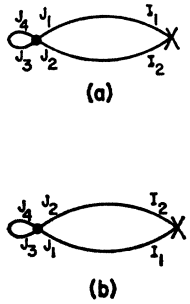

FIG. 1. Example of a labeled diagram. Figures (a) and (b) are the *same* diagram.

the vertex indices, namely,

$$\frac{-\beta}{4!}\sum_{\alpha\beta}\kappa_\alpha\kappa_\beta\sum_{J_1J_2J_3J_4}V_{J_1J_2J_3J_4}\langle u_{J_3}u_{J_4}\rangle^0 \times\langle u_{J_1}u_0{}^\alpha\rangle^0\langle u_{J_2}u_0{}^\beta\rangle^0. \quad (2.20)$$

Different pairings, that is, different labeled diagrams, may have the same *structure* as, for example, when one of the labels J_2, J_3, or J_4 is interchanged with J_1 in Fig. 1(a). These diagrams are topologically equivalent when the labels are omitted and give the same numerical contribution, so that the contribution of a labeled diagram needs only to be multiplied by the number of equivalent diagrams which occur for that structure. To determine this number, consider a general labeled diagram with a κ vertex of order j_0 with m_0 bubbles attached to it and with k V vertices, the ith vertex being of order j_i with m_i bubbles attached to it, $1\leq i\leq k$. Permuting the labels of the points of a vertex leads to diagrams of the same structure and to possibly different pairings of the displacements in (2.18) or its generalization. This introduces first the factor $j_i!$ for that vertex $(0\leq i\leq k)$, then the reduction factor $(\frac{1}{2})^{m_i}$ excluding interchanges of the labels of each bubble and the factor $1/m_i!$ for excluding permutations of the bubbles. Furthermore, if P_{ij} lines connect the vertex pair (ij), there is the reduction factor $1/P_{ij}!$.

If a vertex of order $s(\geq 3)$ occurs r_s times in a diagram, the $r_s!$ permutations among them will give new pairings, with the possible reduction by a *symmetry factor* $1/f_s$.

In the kth order of perturbation being considered, the multinomial factor

$$k!/\prod_{s\geq 3}r_s!$$

is the number of different ways in which the sets of r_s vertex terms $(\sum_{s\geq 3}sr_s=k)$ occur in the expansion

$$(V_A)^k=(\sum_{s\geq 3}V_s)^k.$$

The $r_s!$ cancel out and $k!$ cancels with $1/k!$ in (2.18).

The rules for finding the contribution from diagrams of a given structure can be summarized[10]:

(a) Each V vertex gives the factor $(-\beta)$ times the corresponding CP.

(b) Each line or bubble gives the factor $\langle u_{J_1}u_{J_2}\rangle^0$. If J is on a V vertex,

$$J\rightarrow\binom{\alpha_j}{l_j},$$

and if it is on a κ vertex,

$$J\rightarrow\binom{\alpha}{0}.$$

(c) For each point in (2) on a κ vertex write κ_α.

(d) Sum over all nonfixed indices.

(e) Multiply by the factor

$$(\prod_{i=0}^{k}m_i!\prod_{(ij)}P_{ij}!2^{m_0+m_1+\cdots+m_k}f)^{-1}, \quad (2.21)$$

where f is the product of the symmetry factors. The symmetry factor f is 2 for Figs. 2(a), 2(c), 3(d), 3(f), and 4(b). It is unity for the others.

In the diagram scheme above the quantity $\langle(\boldsymbol{\kappa}\cdot\mathbf{u}_0)^{j_0}\rangle^0$ will involve j_0-order κ vertices. An alternative scheme is to represent each $\boldsymbol{\kappa}\cdot\mathbf{u}_0$ point as a one-point vertex or, equivalently, as an external point. Then we may apply the linked-cluster theorem[9,11] in the forms

$$\langle e^{-\beta V_A}\rangle^0=\exp\langle e^{-\beta V_A}-1\rangle_C{}^0,$$
$$\langle e^{-\beta V_A'}\rangle^0=\exp\langle e^{-\beta V_A'}-1\rangle_{C'}{}^0,$$

where

$$-\beta V_A'\equiv-\beta V_A+i\boldsymbol{\kappa}\cdot\mathbf{u}_0,$$

and the subscripts C and C' denote the restriction to diagrams consisting of connected sets of vertices for V_A and V_A', respectively. The connected diagrams for the latter are of two types: (a) those with no $\boldsymbol{\kappa}\cdot\mathbf{u}_0$ vertex and

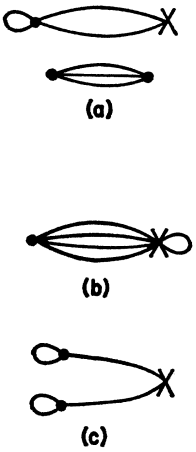

FIG. 2. Examples of unlinked or disconnected diagrams. Figure 2(a) is unlinked and disconnected; Figs. 2(b) and 2(c) are linked and disconnected.

[10] These rules are consistent with those given by W. Götze [Phys. Rev. **156**, 951 (1967)] for the diagrammatic expansion of the vibrational free energy and temperature Green's functions of an anharmonic crystal. At high temperatures $\beta=1/k_BT$ is small and his propagators $\langle T_\tau\{u_{J_1}(\tau)u_{J_2}(0)\}\rangle^0$, $0<\tau<\beta$, are replaced by the pair correlations used here, while each of his integrals $\int_0^\beta d\tau$ gives a factor β. The points of the κ vertex correspond to external points in the Götze article.

[11] J. J. J. Kokkedee, in *Lattice Dynamics*, edited by R. F. Wallis (Pergamon Press, Inc., New York, 1965).

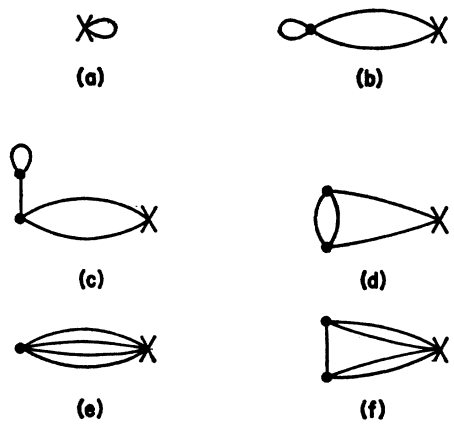

FIG. 3. Lowest-order contributions to the Debye-Waller factor. Figure 3(a) represents the harmonic part; Figs. 3(b) and 3(e) are $O(V_4)$; Figs. 3(c), 3(d), and 3(f) are $O(V_3^2)$, but 3(c) gives no contribution.

(b) those with, which will be denoted by a subscript L. Then

$$\langle e^{-\beta V_A'}\rangle^0=\exp(\langle e^{-\beta V_A}-1\rangle_C{}^0+\langle e^{-\beta V_A+i\kappa\cdot u_0}-1\rangle_{C,L}{}^0)$$

and

$$\langle e^{i\kappa\cdot u_0}\rangle=\langle e^{-\beta V_A+i\kappa\cdot u_0}\rangle^0/\langle e^{-\beta V_A}\rangle^0$$
$$=\exp\langle e^{-\beta V_A-i\kappa\cdot u_0}-1\rangle_{C,L}. \quad (2.22)$$

Returning to our diagram scheme with higher-order κ vertices, we will call a diagram with a κ vertex *linked* (L) if all parts connect to the κ vertex. A diagram with or without a κ vertex will be called *connected* (C) if it is connected without the κ vertex. Then (2.22) still holds with the subscripts having their present meaning. For example, Fig. 2(a) is unlinked and disconnected; Figs. 2(b) and 1(c) are linked and disconnected; Figs. 3 are linked and connected.

By comparing the expressions (2.4) and (2.22) one sees that

$$\langle(i\kappa\cdot\mathbf{u}_0)^n\rangle_{\rm cum}=\langle(i\kappa\cdot\mathbf{u}_0)^n e^{-\beta V_A}\rangle_{C,L}{}^0, \quad (2.23)$$

which is the basis of the subsequent calculations. Furthermore, diagrams with a part connected to other parts by a single line give no contribution in the case of inversion symmetry (see Sec. IV).

III. HARMONIC PAIR-CORRELATION FUNCTIONS

Properties of the Pair-Correlation Function and Relation to the Dynamical Matrix

Use of the symmetry properties of $\langle u_{l_1}{}^{\alpha_1}u_{l_2}{}^{\alpha_2}\rangle^0$ and of its asymptotic properties for large separations reduces the perturbation series of the previous section Displacement invariance gives

$$\langle u_{l_1}{}^{\alpha_1}u_{l_2}{}^{\alpha_2}\rangle^0=\langle u_l{}^{\alpha_1}u_0{}^{\alpha_2}\rangle^0, \quad (3.1)$$

where $\mathbf{l}=\mathbf{l}_1-\mathbf{l}_2$, and inversion symmetry at an atom site gives

$$\langle u_l{}^{\alpha_1}u_0{}^{\alpha_2}\rangle^0=\langle u_{-l}{}^{\alpha_1}u_0{}^{\alpha_2}\rangle^0=\langle u_0{}^{\alpha_1}u_l{}^{\alpha_2}\rangle^0=\langle u_l{}^{\alpha_2}u_0{}^{\alpha_1}\rangle^0. \quad (3.2)$$

Under symmetry rotations $\langle u_{l_1}{}^{\alpha_1}u_{l_2}{}^{\alpha_2}\rangle^0$ transforms like a tensor, so that, if $\mathcal{T}\mathbf{R}_l=\mathbf{R}_{l'}$,

$$\langle u_{l'}{}^{\alpha_1}u_0{}^{\alpha_2}\rangle^0=\sum_{\beta_1,\beta_2=1}^{3}T_{\alpha_1\beta_1}T_{\alpha_2\beta_2}\langle u_l{}^{\beta_1}u_0{}^{\beta_2}\rangle^0. \quad (3.3)$$

In terms of the phonon variables,

$$C_l{}^{\alpha\beta}\equiv\langle u_l{}^{\alpha}u_0{}^{\beta}\rangle^0=\frac{1}{N}\sum_{\mathbf{q}j}\frac{\epsilon_{\mathbf{q}j}{}^{\alpha}\epsilon_{\mathbf{q}j}{}^{\beta*}}{M\omega_{\mathbf{q}j}{}^2}\mathcal{E}(\omega_{\mathbf{q}j}{}^2;T)e^{i\mathbf{q}\cdot\mathbf{R}_l}, \quad (3.4)$$

where $\boldsymbol{\epsilon}_{\mathbf{q}j}$ and $\omega_{\mathbf{q}j}$ are the polarization vector and frequency of the mode $\mathbf{q}j$, and

$$\mathcal{E}(\omega_{\mathbf{q}j}{}^2;T)=\tfrac{1}{2}\hbar\omega_{\mathbf{q}j}\coth\frac{\hbar\omega_{\mathbf{q}j}}{2k_BT}$$
$$=k_BT\left[1-\sum_{n=1}^{\infty}(-1)^n\frac{B_n}{(2n)!}\left(\frac{\hbar\omega_{\mathbf{q}j}}{k_BT}\right)^{2n}\right] \quad (3.5)$$

is its mean energy. The Thirring expansion[12] on the second line of Eq. (3.5) converges for $\hbar\omega_{\mathbf{q}j}/k_BT<2\pi$. The B_n are the Bernoulli numbers, the first three of which are

$$B_1=1/6,\quad B_2=1/30,\quad B_3=1/42. \quad (3.6)$$

The frequencies and polarization vectors are eigenvalues and eigenvectors of the dynamical matrix

$$\sum_{\beta}D(\mathbf{q})^{\alpha\beta}\epsilon_{\mathbf{q}j}{}^{\beta}=\epsilon_{\mathbf{q}j}{}^{\alpha}\omega_{\mathbf{q}j}{}^2, \quad (3.7)$$

where

$$D(\mathbf{q})^{\alpha\beta}=M^{-1}\sum_l V_{l0}{}^{\alpha\beta}e^{-i\mathbf{q}\cdot\mathbf{R}_l}$$
$$=-M^{-1}\sum_l V_{l0}{}^{\alpha\beta}[1-\cos(\mathbf{q}\cdot\mathbf{R}_l)]. \quad (3.8)$$

The eigenvector representation of $D(\mathbf{q})^{\alpha\beta}$ leads to

$$f(D(\mathbf{q}))^{\alpha\beta}=\sum_{j=1}^{3}f(\omega_{\mathbf{q}j}{}^2)\epsilon_{\mathbf{q}j}{}^{\alpha}\epsilon_{\mathbf{q}j}{}^{\beta*}, \quad (3.9)$$

so that Eq. (3.4) can be written

$$C_l{}^{\alpha\beta}=\frac{1}{MN}\sum_{\mathbf{q}}[D^{-1}(\mathbf{q})\mathcal{E}(D(\mathbf{q}))]^{\alpha\beta}e^{i\mathbf{q}\cdot\mathbf{R}_l}, \quad (3.10)$$

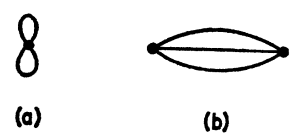

FIG. 4. Lowest-order anharmonic contributions to the Helmholtz free energy.

[12] M. Blackman, *Handbuch der Physik*, edited by S. Flügge (Springer-Verlag, Berlin, 1955), p. 335.

Our calculations apply to the region $T\sim\Theta$ where the quantum corrections are small but not negligible (see, e.g., Table VIII). Then the first two terms of the expansion of $\mathcal{E}(\omega^2)$ are sufficient, and Eq. (3.10) is more convenient than Eq. (3.4) because it is not necessary to solve the eigenvalue problem (3.7), nor to perform the sum over j. At high temperatures,

$$C_l^{\alpha\beta}\xrightarrow[T\sim\Theta_D]{}\frac{k_BT}{MN}\sum_{\mathbf{q}}D^{-1}(\mathbf{q})^{\alpha\beta}e^{i\mathbf{q}\cdot\mathbf{R}_l}+\delta_{\alpha\beta}\delta_{l0}\frac{\hbar^2}{12k_BTM}-\cdots. \quad (3.11)$$

The quantum correction to $C_l^{\alpha\beta}$ is a multiple of the unit matrix and is needed only for the zeroth-order term of (2.8), $\langle(\boldsymbol{\kappa}\cdot\mathbf{u}_0)^2\rangle^0$, so that it will be ignored in the subsequent discussion of the anharmonic contributions. Then

$$C_l^{\alpha\beta}=\frac{k_BTv_c}{8\pi^3M}\int_{\mathrm{BZ}}d^3q\,D^{-1}(\mathbf{q})^{\alpha\beta}e^{i\mathbf{q}\cdot\mathbf{R}_l}, \quad (3.12)$$

where v_c is the unit-cell volume. Since $\mathbf{D}^{-1}$ is real and even in $\mathbf{q}$, $e^{i\mathbf{q}\cdot\mathbf{R}_l}$ can be replaced by $\cos(\mathbf{q}\cdot\mathbf{R}_l)$, and $C_l^{\alpha\beta}$ is real.

Asymptotic Behavior of the Pair Correlation for Large Separations

The behavior of $C_l^{\alpha\beta}$ for large l was considered first by Davies,[13] but the expression derived in this section is much simpler than his. Afterwards we discovered that Flinn and Maradudin[14] had used the first term of the asymptotic expansion in a different context involving crystalline defects. The connection is that the integral in (3.12) is the displacement Green's function of zero frequency and gives the static displacement response at l to a unit force applied at the origin. We will also use the second term in the asymptotic expansion. Comparison with $C_l^{\alpha\beta}$ calculated using Eq. (3.12) will be made in Sec. VII.

In what follows, the notation is for a cubic crystal, but there is no restriction in principle to this symmetry. We introduce the dimensionless variables $\mathbf{k}=a\mathbf{q}/2\pi$ and $\boldsymbol{\varrho}_l=2\mathbf{R}_l/a$ where a is the cube edge. A 3×3 matrix notation will be used for $C^{\alpha\beta}$ and $D^{\alpha\beta}$. Since $\mathbf{D}$ is even in $\mathbf{k}$ and is proportional to k^2 as $k\to0$, $\mathbf{D}^{-1}$ can be written in the form

$$\mathbf{D}^{-1}\left(\frac{2\pi}{a}\mathbf{k}\right)=\sum_{n=-1}^{\infty}\mathbf{f}_{2n}(\hat{k})k^{2n}. \quad (3.13)$$

The matrices $\mathbf{f}_{2n}$ depend on the direction of $\mathbf{k}$. Inserting this expression into Eq. (3.12) and changing variables to a set with k_3' along $\boldsymbol{\varrho}_l$ gives

$$\begin{aligned}\mathbf{C}^l&=\frac{k_BT}{4M}\sum_{n=-1}^{\infty}\int d\Omega'\,\mathbf{f}_{2n}(\hat{k}')\times\tfrac{1}{2}\int_{-K(\hat{k}')}^{K(k')}dk\,k^{2n+2}e^{i\pi k\rho_l\mu'}\\&=\frac{k_BT}{4M}\sum_{n=-1}^{\infty}\int d\Omega'\,\mathbf{f}_{2n}(\hat{k}')\frac{1}{2(i\pi\rho_l)^{2n+2}}\frac{\partial^{2n+2}}{\partial\mu'^{2n+2}}\times\int_{-K(\hat{k}')}^{K(\hat{k}')}dke^{i\pi k\rho_l\mu'}. \quad (3.14)\end{aligned}$$

Here $K(\hat{k}')$ is the length of the vector from the origin to the Brillouin-zone boundary in the direction $\hat{k}'$, $d\Omega'$ is the element of solid angle, and $\mu'=\cos(\hat{k}'\cdot\hat{z})$. Using the asymptotic relation

$$\int_{-K}^{K}e^{i\pi k\rho\mu}dk=\frac{1}{\rho}\int_{-K\rho}^{K\rho}e^{i\pi\mu\chi}d\chi\xrightarrow[\rho\to\infty]{}\frac{2}{\rho}\delta(\mu) \quad (3.15)$$

and, for A and B positive,

$$\int_{-A}^{B}f(\chi)\frac{d^n\delta(\chi)}{d\chi^n}d\chi=(-1)^n\frac{d^nf(\chi)}{d\chi^n}\Big|_{\chi=0} \quad (3.16)$$

in (3.14) gives

$$\mathbf{C}_l\xrightarrow[\rho_l\to\infty]{}\rho_l^{-1}\mathbf{C}^{(1)}(\hat{\rho}_l)+\rho_l^{-3}\mathbf{C}^{(2)}(\hat{\rho}_l)+O(\rho_l^{-5}), \quad (3.17)$$

where

$$\mathbf{C}^{(1)}=\frac{k_BT}{4M}\int d\Omega'\,\mathbf{f}_{-2}(\hat{k}')\delta(\mu') \quad (3.18)$$

and

$$\mathbf{C}^{(2)}=-\frac{k_BT}{4\pi^2M}\int d\Omega'\frac{\partial^2\mathbf{f}_0(\hat{k}')}{\partial\mu'^2}\delta(\mu'). \quad (3.19)$$

The replacement of the χ integral in (3.15) by $\delta(\mu')$ neglects the ρ dependence coming from the limits of integration. In the original integral this is the Brillouin-zone surface. Surface discontinuities can give an oscillatory term like $\rho^{-p}\cos(\pi\mathbf{K}\cdot\boldsymbol{\varrho})$, where p is some power. Such terms occur, for example, in the x-ray scattering factor for a particle of uniform electron density and could alter the asymptotic expansion (3.17) after the first term. However, the Brillouin-zone boundary is *not* a discontinuity for the $\mathbf{r}=\mathbf{R}_l$ ($\boldsymbol{\varrho}=\boldsymbol{\varrho}_l$), since the $\mathbf{k}$ integral is then periodic in k space and the choice of the period-cell boundary is immaterial. The same applies to the neglect of the derivatives of the limits of integration in (3.14).

The matrices $\mathbf{f}_{2n}$ introduced in Eq. (3.13) are found as follows: Expand the matrix $\mathbf{D}$ in a power series:

$$\mathbf{D}=\sum_{n=1}^{\infty}\mathbf{D}_{2n}, \quad (3.20)$$

[13] R. O. Davies and A. V. Reader, in *Proceedings of the Eighth International Conference on Low Temperature Physics, London, 1962*, edited by R. O. Davies (Butterworths Scientific Publications Ltd., London, 1963).

[14] P. A. Flinn and A. A. Maradudin, Ann. Phys. (N. Y.) 18, 81 (1962).

where $\mathbf{D}_{2n}$ is proportional to k^{2n}. Then

$$\begin{aligned}\mathbf{D}^{-1}&=(\sum_{n=1}^{\infty}\mathbf{D}_{2n})^{-1}\\&=(1+\mathbf{D}_2^{-1}\sum_{n=2}^{\infty}\mathbf{D}_{2n})^{-1}\mathbf{D}_2^{-1}\\&=[1-\mathbf{D}_2^{-1}\sum_{n=2}^{\infty}\mathbf{D}_{2n}+(\mathbf{D}_2^{-1}\sum_{n=2}^{\infty}\mathbf{D}_{2n})^2-\cdots]\mathbf{D}_2^{-1}\\&=\mathbf{D}_2^{-1}-\mathbf{D}_2^{-1}\mathbf{D}_4\mathbf{D}_2^{-1}+O(k^2)\\&=\mathbf{f}_{-2}/k^2+\mathbf{f}_0+O(k^2).\end{aligned}\tag{3.21}$$

Since $\mathbf{D}_{2n}\propto k^{2n}$, it follows that

$$\mathbf{f}_{-2}=k^2\mathbf{D}_2^{-1}\tag{3.22}$$

and

$$\mathbf{f}_0=-\mathbf{D}_2^{-1}\mathbf{D}_4\mathbf{D}_2^{-1}.\tag{3.23}$$

IV. DEBYE-WALLER ANHARMONIC TERMS FOR A CUBIC CRYSTAL

Enumeration of the Linked-Cluster Sums Needed

Only connected linked diagrams contribute to the cumulants $\langle(\boldsymbol{\kappa}\cdot\mathbf{u}_0)^n\rangle_{\rm cum}$ (see Sec. II). Each such diagram will be denoted by $\mathfrak{L}$, so that the Debye-Waller factor (2.4) contains

$$\langle(\boldsymbol{\kappa}\cdot\mathbf{u}_0)^{2n}\rangle_{\rm cum}=\sum_{\mathfrak{L}}\langle e^{-\beta V_A}(\boldsymbol{\kappa}\cdot\mathbf{u}_0)^{2n}\rangle_{\mathfrak{L}^0},\quad n=1,2,\cdots.\tag{4.1}$$

The first terms in the perturbation expansion are obtained from terms in V_4 and V_3^2 which give contributions of the same order of magnitude. The question arises as to which are larger, the first-order contributions to κ^4 or the higher-order, i.e., V_6 and V_3V_5, contributions to κ^2. An estimate can be based on the assumption that $V_{n+2}\sim(u^n/d^n)V_2$, where d is a length which characterizes the rate of change, of say, the repulsive interaction. (For a Born-Mayer potential, $d\sim\frac{1}{10}R_{\rm nn}$, where $R_{\rm nn}$ is the nearest-neighbor distance.) Thus $\langle\mathbf{u}^2\rangle^0/d^2$ is the perturbation parameter and one obtains the following expansions:

$$\begin{aligned}&\tfrac{1}{2}\kappa^2\langle\mathbf{u}_0^2\rangle\sim\tfrac{1}{2}\kappa^2\langle\mathbf{u}_0^2\rangle^0\left(1+A\frac{\langle\mathbf{u}_0^2\rangle^0}{d^2}+B\frac{(\langle\mathbf{u}_0^2\rangle^0)^2}{d^4}+\cdots\right),\\&\frac{\kappa^4}{4!}[\langle\mathbf{u}_0^4\rangle-3\langle\mathbf{u}_0^2\rangle^2]\sim\frac{3\kappa^4}{4!}(\langle\mathbf{u}_0^2\rangle^0)^2\left(A'\frac{\langle\mathbf{u}_0^2\rangle^0}{d^2}+B'\frac{(\langle\mathbf{u}_0^2\rangle^0)^2}{d^2}+\cdots\right).\end{aligned}\tag{4.2}$$

The coefficients A, A', B, and B' are presumed to be of order unity. The ratio of the κ^2 terms of higher order to the κ^4 terms of first order is $4B/A'\kappa^2d^2$. When $\kappa^2\langle\mathbf{u}_0^2\rangle^0\sim1$, as it must be if the Debye-Waller factor is to be important, then $\kappa^2d^2\sim20$ and the ratio becomes $B/5A'$, so that these terms are about the same order of magnitude. Since part of the κ^4 terms are nonisotropic, an effect which cannot be cancelled out by the κ^2 terms of second, order we have chosen to calculate, besides the κ^2 terms of first order, the κ^4 terms of first order. In the numerical work V_A then, was restricted to be V_3+V_4.

We will now restrict ourselves to the consideration of cubic crystals. Expanding the exponential in Eq. (4.1) and keeping terms of order V_4 and V_3^2, one obtains for $n=1$

$$\begin{aligned}\tfrac{1}{2}\langle(\boldsymbol{\kappa}\cdot\mathbf{u}_0)^2\rangle_{\rm cum}&=\tfrac{1}{2}[\langle(\boldsymbol{\kappa}\cdot\mathbf{u}_0)^2\rangle^0-\beta\sum_{\mathfrak{L}}\langle V_4(\boldsymbol{\kappa}\cdot\mathbf{u}_0)^2\rangle_{\mathfrak{L}^0}\\&\quad+\tfrac{1}{2}\beta^2\sum_{\mathfrak{L}}\langle V_3^2(\boldsymbol{\kappa}\cdot\mathbf{u}_0)^2\rangle_{\mathfrak{L}^0}]\\&\equiv M_0+M_1+M_2,\end{aligned}\tag{4.3}$$

respectively. For a cubic crystal $\langle(\boldsymbol{\kappa}\cdot\mathbf{u}_0)^2\rangle$ may be replaced by $\frac{1}{3}\kappa^2\langle\mathbf{u}_0^2\rangle$.

The diagram associated with M_0 is shown in Fig. 3(a) and its contribution is

$$\tfrac{1}{2}\sum_{\alpha\beta}\kappa_\alpha\kappa_\beta\langle u_0^\alpha u_0^\beta\rangle^0=\tfrac{1}{6}\kappa^2\langle\mathbf{u}_0^2\rangle^0.\tag{4.4}$$

The M_1 diagram is shown in Fig. 3(b), and the associated contribution is,

$$\begin{aligned}M_1&=-\tfrac{1}{4}\beta\kappa^2\sum V_{l_1l_2l_3l_4}{}^{\alpha_1\alpha_2\alpha_3\alpha_4}C_{l_1}{}^{\alpha_1 1}C_{l_2}{}^{\alpha_2 1}C_{l_3-l_4}{}^{\alpha_3\alpha_4}\\&=-\tfrac{1}{12}\beta\kappa^2\sum V_{l_1l_2l_3l_4}{}^{\alpha_1\alpha_2\alpha_3\alpha_4}C_{l_1}{}^{\alpha_1\mu}\\&\qquad\times C_{l_2}{}^{\alpha_2\mu}C_{l_3-l_4}{}^{\alpha_3\alpha_4}.\end{aligned}\tag{4.5}$$

The sum in the second line runs over all repeated indices.

With M_2 are associated the diagrams in Figs. 3(c) and 3(d). The contribution of the diagram of Fig. 3(c) is zero because of inversion symmetry. To see this, consider

$$\begin{aligned}&\sum V_{l_1l_2l_3}{}^{\alpha_1\alpha_2\alpha_3}V_{l_4l_5l_6}{}^{\alpha_4\alpha_5\alpha_6}C_{l_1-l_2}{}^{\alpha_1\alpha_2}C_{l_3-l_4}{}^{\alpha_3\alpha_4}\\&\qquad\times C_{l_5}{}^{\alpha_5 1}C_{l_6}{}^{\alpha_6 1}.\end{aligned}\tag{4.6}$$

Displacement invariance [Eqs. (2.13a) and (3.1)] permits replacing the first and third factors in (4.6) by

$$V_{l_1'l_2'0}{}^{\alpha_1\alpha_2\alpha_3}C_{l_1'-l_2'}{}^{\alpha_1\alpha_2},\quad l_i'=l_i-l_3,\quad i=1,2$$

which, together with the relations

$$C_{-(l_1'-l_2')}{}^{\alpha_1\alpha_2}=C_{l_1'-l_2'}{}^{\alpha_1\alpha_2}$$

and

$$V_{-l_1',-l_2',0}{}^{\alpha_1\alpha_2\alpha_3}=-V_{l_1'l_2'0}{}^{\alpha_1\alpha_2\alpha_3}$$

from (3.2) and (2.13c), respectively, shows that the l_1', l_2' sum in (4.6) gives zero. This argument holds for any diagram containing a part joined to the rest by a single line, since all other points in that part may be measured from the point of attachment of the line and these other points, being end points of lines, are even in number.

The contribution associated with Fig. 3(d) is, for a cubic crystal,

$$M_2=\tfrac{1}{12}\beta^2\kappa^2\sum V_{l_1l_2l_3}{}^{\alpha_1\alpha_2\alpha_3}V_{l_4l_5l_6}{}^{\alpha_4\alpha_5\alpha_6}C_{l_1-l_4}{}^{\alpha_1\alpha_4}\times C_{l_2-l_5}{}^{\alpha_2\alpha_5}C_{l_3}{}^{\alpha_3\mu}C_{l_6}{}^{\alpha_6\mu}. \quad (4.7)$$

The κ^4 term is

$$\begin{aligned}\langle(\boldsymbol{\kappa}\cdot\mathbf{u}_0)^4\rangle_{\rm cum}&=\sum_{\mathcal{L}}\langle e^{-\beta V_A}(\boldsymbol{\kappa}\cdot\mathbf{u}_0)^4\rangle_{\mathcal{L}}{}^0\\&=-\beta\sum_{\mathcal{L}}\langle V_4(\boldsymbol{\kappa}\cdot\mathbf{u}_0)^4\rangle_{\mathcal{L}}{}^0\\&\quad+\tfrac{1}{2}\beta^2\sum_{\mathcal{L}}\langle V_3{}^2(\boldsymbol{\kappa}\cdot\mathbf{u}_0)^4\rangle_{\mathcal{L}}{}^0\\&\equiv M_3+M_4, \quad (4.8)\end{aligned}$$

since $\langle(\boldsymbol{\kappa}\cdot\mathbf{u})^n\rangle^0{}_{\rm cum}=0$ for $n>2$ according to the remark below Eqs. (2.3). Again, only terms containing V_4 and $V_3{}^2$ are kept.

The diagram associated with M_3 is shown in Fig. 3(e), and the contribution is

$$M_3=\frac{\beta}{4!}\sum\kappa_\alpha\kappa_\beta\kappa_\gamma\kappa_\delta\Big(\sum V_{l_1l_2l_3l_4}{}^{\alpha_1\alpha_2\alpha_3\alpha_4}C_{l_1}{}^{\alpha_1\alpha}\times C_{l_2}{}^{\alpha_2\beta}C_{l_3}{}^{\alpha_3\gamma}C_{l_4}{}^{\alpha_4\delta}\Big). \quad (4.9)$$

The κ sum can be simplified for a cubic crystal. We write

$$M_3=\sum\kappa_\alpha\kappa_\beta\kappa_\gamma\kappa_\delta\,\mathfrak{M}_3{}^{\alpha\beta\gamma\delta},$$

with $\mathfrak{M}_3{}^{\alpha\beta\gamma\delta}$ equal to the term in parenthesis of Eq. (4.9), and note that (a) $\mathfrak{M}_3$ is symmetrical in its four indices, (b) the transformation $x\rightarrow -x$ requires that a Cartesian index occur an even number of times, and (c) all cubic symmetry operations permute tensor indices with possible sign changes. Therefore, the two distinct nonzero elements of $\mathfrak{M}_3$ are of the form $\mathfrak{M}_3{}^{\alpha\alpha\beta\beta}$ ($=\mathfrak{M}_3{}^{\alpha\beta\alpha\beta}$, etc.), $\alpha\neq\beta$, and $\mathfrak{M}_3{}^{\alpha\alpha\alpha\alpha}$. If we define

$$\mathfrak{M}_3{}^{11}\equiv\mathfrak{M}_3{}^{\alpha\alpha\alpha\alpha}, \quad \mathfrak{M}_3{}^{12}\equiv 3\mathfrak{M}_3{}^{\alpha\alpha\beta\beta}, \quad (4.10)$$

then M_3 can be written

$$M_3=\mathfrak{M}_3{}^{11}\sum_\alpha\kappa_\alpha{}^2+\mathfrak{M}_3{}^{12}\sum_{\alpha\beta}{}'\kappa_\alpha{}^2\kappa_\beta{}^2, \quad (4.11)$$

where the prime on the summation means to omit those terms for which $\alpha=\beta$. Alternatively, M_3 can be written as the sum of an isotropic part and of a part proportional to the invariant cubic harmonic, $h_1\equiv\frac{5}{2}\,(\sum_\alpha\kappa_\alpha{}^4/\kappa^4-\frac{3}{5})$, which averages to zero over solid angle and gives the deviation from isotropy,

$$M_3=\kappa^4[\tfrac{3}{5}(\mathfrak{M}_3{}^{11}+\tfrac{2}{3}\mathfrak{M}_3{}^{12})+\tfrac{5}{2}(\mathfrak{M}_3{}^{11}-\mathfrak{M}_3{}^{12})h_1]. \quad (4.12)$$

The diagram associated with M_4 is shown in Fig. 3(f). Its contribution is

$$\begin{aligned}M_4&=-\tfrac{1}{8}\beta^2\sum\kappa_\alpha\kappa_\beta\kappa_\gamma\kappa_\delta\Big(V_{l_1l_2l_3}{}^{\alpha_1\alpha_2\alpha_3}V_{l_4l_5l_6}{}^{\alpha_4\alpha_5\alpha_6}\\&\quad\times C_{l_1}{}^{\alpha_1\alpha}C_{l_2}{}^{\alpha_2\beta}C_{l_4}{}^{\alpha_4\gamma}C_{l_5}{}^{\alpha_5\delta}C_{l_3-l_6}{}^{\alpha_3\alpha_6}\Big)\\&\equiv\sum\kappa_\alpha\kappa_\beta\kappa_\gamma\kappa_\delta\mathfrak{M}_4{}^{\alpha\beta\gamma\delta}. \quad (4.13)\end{aligned}$$

Although $\mathfrak{M}_4{}^{\alpha\beta\gamma\delta}$ defined by the sum in parentheses in (4.13) is not symmetrical in its four indices, only the quantities

$$\mathfrak{M}_4{}^{11}\equiv\mathfrak{M}_4{}^{\alpha\alpha\alpha\alpha}, \quad \mathfrak{M}_4{}^{12}\equiv\mathfrak{M}_4{}^{\alpha\alpha\beta\beta}+2\mathfrak{M}_4{}^{\alpha\beta\alpha\beta} \quad (4.14)$$

are needed and

$$\begin{aligned}M_4&=\mathfrak{M}_4{}^{11}\sum_\alpha\kappa_\alpha{}^2+\mathfrak{M}_4{}^{12}\sum_{\alpha\beta}{}'\kappa_\alpha{}^2\kappa_\beta{}^2,\\&=\kappa^2[\tfrac{3}{5}(\mathfrak{M}_4{}^{11}+\tfrac{2}{3}\mathfrak{M}_4{}^{12})+\tfrac{2}{5}(\mathfrak{M}_4{}^{11}-\mathfrak{M}_4{}^{12})h_1]. \quad (4.15)\end{aligned}$$

Convergence Rates of Sums

The sums involved in calculation of the anharmonic contributions to the Debye-Waller factor can be written in a way which makes their convergence properties more apparent. The greatest contribution to the anharmonic coupling parameters comes from the short-range part of the potential, so that each third- and fourth-order CP decreases rapidly as the difference $|\mathbf{l}-\mathbf{l}'|$ for any two arguments becomes large. The sums can be rewritten so that each CP has an argument $l=0$ and the other arguments are then restricted to a neighborhood of zero.

The M_1 sum (4.5) becomes

$$M_1=-\tfrac{1}{12}\beta\kappa^2\sum_{\substack{l_1,l_2,l_3\\ \alpha_1,\alpha_2,\alpha_3,\alpha_4}}V_{l_1l_2l_30}{}^{\alpha_1\alpha_2\alpha_3\alpha_4}C_{l_3}{}^{\alpha_3\alpha_4}\times\sum_{l_4,\mu}C_{l_1+l_4}{}^{\alpha_1\mu}C_{l_2+l_4}{}^{\alpha_2\mu}. \quad (4.16)$$

The sum over l_4 is not absolutely convergent because $C_{l_1+l_4}\sim\rho_{l_4}{}^{-1}$ asymptotically, but it can be made to converge by replacing the inner sum by $-B_{l_1-l_2}{}^{\alpha_1\alpha_2}$, where

$$\begin{aligned}B_{l_1-l_2}{}^{\alpha_1\alpha_2}&\equiv\sum_{l_4,\mu}(C_{l_4}{}^{\alpha_1\mu}C_{l_4}{}^{\alpha_2\mu}-C_{l_1+l_4}{}^{\alpha_1\mu}C_{l_2+l_4}{}^{\alpha_2\mu})\\&=\sum_{l_4,\mu}[C_{l_4}{}^{\alpha_1\mu}C_{l_4}{}^{\alpha_2\mu}-\tfrac{1}{2}(C_{l_1+l_4}{}^{\alpha_1\mu}C_{l_2+l_4}{}^{\alpha_2\mu}\\&\quad+C_{-l_1+l_4}{}^{\alpha_1\mu}C_{-l_2+l_4}{}^{\alpha_2\mu})], \quad (4.17)\end{aligned}$$

where use has been made of the symmetry (3.2). The summand on the last line of (4.17) decreases as $\rho_{l_4}{}^{-4}$ for large ρ_{l_4}. This can be seen by expanding it in a Taylor series about $l_1=l_2=0$. Introducing (4.17) into (4.16) does not change the latter value because the sum over l_1, using (2.13a), shows that the added term is zero.

Even with the $\rho_{l_4}{}^{-4}$ dependence in (4.17) the sum over l_4 would have to be taken to $\rho_{l_4}\sim 100$ for 1% accuracy. It proved more expedient to evaluate $\mathbf{B}_l$ as a Brillouin-zone integral. Using the first term on the right side of (3.11) for $\mathbf{C}_l$ and the relation

$$\sum_{l_4}\exp[i(\mathbf{q}_1+\mathbf{q}_2)\cdot\mathbf{R}_{l_4}]=N\delta_{\mathbf{q}_1,-\mathbf{q}_2}$$

for $\mathbf{q}_{1,2}$ inside the Brillouin zone, we obtain

$$B_l^{\alpha_1\alpha_2}=\frac{(k_BT)^2}{NM^2}\sum_{\mathbf{q},\mu}[D^{-1}(\mathbf{q})]^{\alpha_1\mu}[D^{-1}(\mathbf{q})]^{\mu\alpha_2}\times[1-\cos(\mathbf{q}\cdot\mathbf{R}_l)]$$
$$=\frac{(k_BT)^2}{4M^2}\int_{\mathrm{BZ}}d^3k\,[1-\cos(\pi\mathbf{k}\cdot\boldsymbol{\varrho}_l)]\times\sum_{\mu}\left[D^{-1}\left(\frac{2\pi\mathbf{k}}{a}\right)\right]^{\alpha_1\mu}\left[D^{-1}\left(\frac{2\pi\mathbf{k}}{a}\right)\right]^{\mu\alpha_2}. \quad (4.18)$$

The integrand has a k^{-2} singularity at $\mathbf{k}=0$, so that the same integration procedure was used as for the evaluation of $\mathbf{C}_l$ from Eq. (3.12). The convergence of the sum

$$M_1=\tfrac{1}{12}\beta\kappa^2\sum V_{l_1l_2l_30}{}^{\alpha_1\alpha_2\alpha_3}C_{l_3}{}^{\alpha_3\alpha_4\alpha_4}B_{l_1-l_2}{}^{\alpha_1\alpha_2} \quad (4.19)$$

is determined by the (short) range of $V_{l_1l_2l_30}$.

Similar convergence techniques are needed for the sum (4.7) for M_2, where neither the l_3 nor l_6 sums are absolutely convergent. After the transformations $l_{1,2}-l_3\rightarrow l_{1,2}$, $l_{4,5}-l_6\rightarrow l_{4,5}$, and $l_3-l_6\rightarrow l_3$, and doing the l_6 sum using (4.17), we get

$$M_2=-\tfrac{1}{12}\beta\kappa^2\sum V_{l_1l_20}{}^{\alpha_1\alpha_2\alpha_3}V_{l_4l_50}{}^{\alpha_4\alpha_5\alpha_6}C_{l_1-l_4+l_3}{}^{\alpha_1\alpha_4}\times C_{l_2-l_5+l_3}{}^{\alpha_2\alpha_5}B_{l_3}{}^{\alpha_3\alpha_6}. \quad (4.20)$$

Here the indices l_1, l_2, l_4, and l_5 are restricted by the CP to a region about the origin and the convergence rate of the summand is determined by the l_3 sum. To determine this rate we first note that the asymptotic dependence of B_{l_3} on ρ_{l_3} is determined by those terms of $\mathbf{D}^{-1}$ in the integrand of Eq. (4.18) which are proportional to k^{-2}. It will be shown in Sec. VII that $B_l\sim\rho_l$ for large ρ_l. Next, the product $C_{l_1-l_4+l_3}C_{l_2-l_5+l_3}$ is expanded in a Taylor series about $\boldsymbol{\varrho}_{l_1}=\boldsymbol{\varrho}_{l_2}=\boldsymbol{\varrho}_{l_4}=\boldsymbol{\varrho}_{l_5}=0$. The only terms in this expansion which give a nonzero contribution to M_2 are those for which each of the expansion variables $\rho_{l_1}{}^\alpha$, $\rho_{l_2}{}^\alpha$, $\rho_{l_4}{}^\alpha$, and $\rho_{l_5}{}^\alpha$ appears at least once, since otherwise the condition (2.13a) would give zero. On the other hand, $V_{l_1l_30}=-V_{-l_1-l_20}$ [see Eq. (2.13c)], so that the sum of the exponents of $\rho_{l_1}{}^\alpha$ and $\rho_{l_2}{}^\beta$ must be odd for the summand to be even. The same applies to $\rho_{l_4}{}^\alpha$ and $\rho_{l_5}{}^\beta$. Therefore, the number of partial derivatives with respect to components of $\boldsymbol{\varrho}_{l_3}$ must be even so that the resulting function is even in $\boldsymbol{\varrho}_{l_3}$ (note that $\mathbf{B}_{l_3}$ is even in $\boldsymbol{\varrho}_{l_3}$). The first term to give a nonvanishing result occurs when the sum of the exponents of $\rho_{l_1}{}^\alpha$ and $\rho_{l_2}{}^\beta$ is 3. The same holds true for $\rho_{l_4}{}^\alpha$ and $\rho_{l_5}{}^\beta$. The products of the third derivatives of the asymptotic expression for C result in a term of order $\rho_{\mathrm{nn}}{}^6\rho_{l_3}{}^{-8}$ and multiplication by $\mathbf{B}_{l_3}$ gives $\rho_{\mathrm{nn}}{}^6\rho_{l_3}{}^{-7}$, where ρ_{nn} refers to the nearest-neighbor distance.

If the l_3 sum is taken over all points within a radius ρ_c, the neglected part will be of order $\rho_{\mathrm{nn}}{}^6\rho_c{}^{-4}$. For accuracy of about 1%, $\rho_c\approx3.2\rho_{\mathrm{nn}}{}^{3/2}\approx5.4$ for an fcc crystal.

Writing $\mathfrak{M}_3{}^{\alpha\beta\gamma\delta}$ so that the fourth-order CP has a zero argument, one obtains

$$\mathfrak{M}_3{}^{\alpha\beta\gamma\delta}=\frac{\beta}{24}\sum V_{l_1l_2l_30}{}^{\alpha_1\alpha_2\alpha_3\alpha_4}C_{l_1+l_4}{}^{\alpha_1\alpha}\times C_{l_2+l_4}{}^{\alpha_2\beta}C_{l_3+l_4}{}^{\alpha_3\gamma}C_{l_4}{}^{\alpha_4\delta}. \quad (4.21)$$

(All indices except α, β, γ, and δ are summed.) The convergence rate with respect to l_4 is determined by expanding each of the $C_{l_i+l_4}$, $i=2, 3, 4$, in a Taylor series about the point $\boldsymbol{\varrho}_{l_i}=0$. Here each of the $\rho_{l_i}{}^\alpha$, $i=1, 2, 3$, must appear, and since $V_{l_1l_2l_30}=V_{-l_1-l_2-l_30}$, the sum of the exponents of the $\rho_{l_i}{}^\alpha$ must be even. The lowest-order term which contributes is of order $\rho_{\mathrm{nn}}{}^4\rho_{l_4}{}^{-7}$ and the neglected part is of order $\rho_{\mathrm{nn}}{}^4\rho_{l_4}{}^{-4}$. For accuracy of about 1% one should choose $\rho_c\approx3.2\rho_{\mathrm{nn}}\approx4.5$ for an fcc crystal.

The arguments used here are similar to those used for calculating the electrostatic potential in an ionic crystal, which also involves conditionally convergent series. Because of the vanishing of the sum (2.13a), the CP are like neutral multipoles. The introduction of $B_l{}^{\alpha_1\alpha_2}$ into (4.16) corresponds to replacing the potentials of the individual charges in a cell by the potential of a multipole.

The most complicated sum, among those considered, for discussing convergence is that for $\mathfrak{M}_4$ in (4.13) which can be written

$$\mathfrak{M}_4{}^{\alpha\beta\gamma\delta}=-\tfrac{1}{8}\beta^2\sum V_{l_1l_20}{}^{\alpha_1\alpha_2\alpha_3}V_{l_4l_50}{}^{\alpha_4\alpha_5\alpha_6}C_{l_1+l_3}{}^{\alpha_1\alpha}\times C_{l_2+l_3}{}^{\alpha_2\beta}C_{l_4+l_6}{}^{\alpha_4\gamma}C_{l_5+l_6}{}^{\alpha_5\delta}C_{l_3-l_6}{}^{\alpha_3\alpha_6}. \quad (4.22)$$

The change in variables $l_{4,5,6}\rightarrow-l_{4,5,6}$, together with $V_{-l_4-l_50}=-V_{l_4l_50}$, leads to the replacement in (4.22),

$$\mathbf{C}_{l_3-l_6}\rightarrow\tfrac{1}{2}(\mathbf{C}_{l_3-l_6}-\mathbf{C}_{l_3+l_6}). \quad (4.23)$$

The double sum over l_3 and l_6 in (4.22) is unrestricted in range by the CP and corresponds in Fig. 3(f) to each of the V vertices being arbitrarily far from the κ vertex. For purposes of estimation the sum may be replaced by an integral ($\rho_{l_{3,6}}>\rho_{\mathrm{nn}}$) equal to twice that over the region $\rho_{l_6}<\rho_{l_3}$, and we consider the error in cutting off the $\boldsymbol{\varrho}_{l_3}$ integration at ρ_c. Using the asymptotic form of the $\mathbf{C}$'s and the Taylor expansion in $\rho_{l_{1,2,4,5}}{}^\alpha$ as for $\mathfrak{M}_3$ leads to the relative error in the ρ_c cutoff of order

$$2\rho_{\mathrm{nn}}{}^5\int_{\rho_c}^{\infty}\frac{d^3\rho_{l_3}}{\rho_{l_3}{}^5}\int_{\rho_{\mathrm{nn}}}^{\rho_{l_3}}\frac{d^3\rho_{l_6}}{\rho_{l_6}{}^5}\frac{1}{2}\left(\frac{1}{|\boldsymbol{\varrho}_{l_3}-\boldsymbol{\varrho}_{l_6}|}-\frac{1}{|\boldsymbol{\varrho}_{l_3}+\boldsymbol{\varrho}_{l_6}|}\right).$$

The region $|\boldsymbol{\varrho}_{l_3}\mp\boldsymbol{\varrho}_{l_6}|\sim\rho_{\mathrm{nn}}$ makes a contribution to the $\boldsymbol{\varrho}_{l_3}$ integrand of order $\rho_{\mathrm{nn}}{}^7\rho_{l_3}{}^{-10}$, so that the relative error is of order $(\rho_{\mathrm{nn}}/\rho_c)^7$. In the remaining region, approximating the expression in parentheses by $2\rho_{l_6}/\rho_{l_3}{}^2$ gives a $\boldsymbol{\varrho}_{l_3}$ integrand $\sim2\rho_{\mathrm{nn}}{}^4\rho_{l_3}{}^{-7}$ and the larger cutoff error of order $\frac{1}{2}(\rho_{\mathrm{nn}}/\rho_c)^4$. To keep this to less than 1% requires summing to $\rho_c\gtrsim2.7\rho_{\mathrm{nn}}\approx4$ for an fcc crystal. Machine calculations show that the estimates above are quite reliable.

V. THERMAL EXPANSION

The treatment follows closely that of Maradudin.[15] The equilibrium positions $\mathbf{R}_l$ are for some reference temperature T_0. Changing T causes strains $\eta_{\alpha\beta}$ and changes in $\mathbf{R}_l$:

$$\xi_l{}^\alpha=\sum_\beta \eta_{\alpha\beta}R_l{}^\beta. \tag{5.1}$$

The changes are due to the anharmonic potential and are proportional to V_3 or V_4, so that, to the order of perturbation V_4 or $V_3{}^2$, only the change in M_0 need be considered. Under the combined displacements $\mathbf{u}_l+\boldsymbol{\xi}_l$, which is equivalent to the displacements $\mathbf{u}_l$ from the new equilibrium positions, the potential energy is

$$V=\sum_{j=0}^{\infty} V_j(u)+\frac{1}{2!}\sum V_{l_1l_2}{}^{\alpha_1\alpha_2}\xi_{l_1}{}^{\alpha_1}u_{l_2}{}^{\alpha_2}u_{l_3}{}^{\alpha_3} +\frac{1}{3!}\sum V_{l_1l_2l_3l_4}{}^{\alpha_1\alpha_2\alpha_3\alpha_4}\xi_{l_1}{}^{\alpha_1}u_{l_2}{}^{\alpha_2}u_{l_3}{}^{\alpha_3}u_{l_4}{}^{\alpha_4} +\cdots+\text{terms in } \xi^2+\cdots. \tag{5.2}$$

The terms linear in both ξ and u vanish, since $\mathbf{R}_l+\boldsymbol{\xi}_l$ are still equilibrium positions. The term in ξuuu vanishes on the average and can only enter squared in a perturbation expansion, so that it is ignored. The new harmonic CP are

$$V_{l_1l_2}{}^{\alpha_1\alpha_2}+\sum_{l_3,\alpha_3} V_{l_1l_2l_3}{}^{\alpha_1\alpha_2\alpha_3}\xi_{l_3}{}^{\alpha_3} =V_{l_1l_2}{}^{\alpha_1\alpha_2}+\sum_{l_3,\alpha_3} V_{l_1l_2l_3}{}^{\alpha_1\alpha_2\alpha_3}(\xi_{l_3}{}^{\alpha_3}-\xi_{l_1}{}^{\alpha_3}), \tag{5.3}$$

where we have made use of (2.13a).

This changes the dynamical matrix (3.8) by

$$\Delta D(\mathbf{q})^{\alpha\beta}=\sum_{\gamma\delta} d(\mathbf{q})^{\alpha\beta,\gamma\delta}\eta_{\gamma\delta}, \tag{5.4}$$

where

$$d(\mathbf{q})^{\alpha\beta,\gamma\delta}=-\frac{1}{M}\sum_{l_1,l_2} V_{l_10l_2}{}^{\alpha\beta\gamma}R_{l_2}{}^{\delta}[1-\cos(\mathbf{q}\cdot\mathbf{R}_{l_1})]. \tag{5.5}$$

The change in M_0 is proportional to $\Delta C_0{}^{\alpha\alpha}$, which, by (3.12), (5.4), and (5.5), is

$$\Delta C_0{}^{\alpha\alpha}=-\frac{k_BTv_c}{8\pi^3M}\sum_{\gamma\delta}\eta_{\gamma\delta}\int_{\mathrm{BZ}} d^3q\sum_\beta (\mathbf{D}^{-1})^{\alpha\beta} \times d^{\beta\beta',\gamma\delta}(\mathbf{D}^{-1})^{\beta'\alpha}. \tag{5.6}$$

For the cubic symmetry $\eta_{\alpha\beta}=\delta_{\alpha\beta}\eta(T)$.

The thermal expansion $\eta(T)$ can be taken from experiment or calculated directly. For the latter, we expand the Helmholtz free energy in $\eta_{\alpha\beta}$ and $T-T_0$, i.e.,

$$F=F_0+F_{0T}(T-T_0)+\sum_{\alpha\beta} F_{0\alpha\beta;T}\eta_{\alpha\beta}(T-T_0) +\tfrac{1}{2}\sum_{\alpha\beta\gamma\delta} F_{0\alpha\beta\gamma\delta}\eta_{\alpha\beta}\eta_{\gamma\delta}+\cdots, \tag{5.7}$$

where $F_{0\alpha\beta\gamma\delta}$ are isothermal elastic compliance coefficients. Minimizing (5.7) with respect to $\eta_{\alpha\beta}$ leads to

$$F_{0\alpha\beta;T}(T-T_0)+\sum_{\gamma\delta} F_{0\alpha\beta\gamma\delta}\eta_{\gamma\delta}=0, \tag{5.8}$$

and, abbreviating the argument about cubic symmetry (see Ref. 15), we get

$$\eta(T)=-\frac{(T-T_0)F_{011;T}}{3\Omega_0B_0{}^{\mathrm{is}}}, \tag{5.9}$$

where Ω_0 is the crystal volume and $B_0{}^{\mathrm{is}}$ is the isothermal bulk modulus at temperatures T_0.

To find

$$F_{0\alpha\beta;T}\equiv\left.\frac{\partial^2F}{\partial\eta_{\alpha\beta}\partial T}\right|_{T_0,\mathbf{R}_l}, \tag{5.10}$$

we use the relation[9]

$$\delta F=\langle\delta H\rangle+O\{(\delta H)^2\},$$

and restrict ourselves, for the accuracy required, to δF_{harm}:

$$F_{\mathrm{harm},\alpha\beta}\equiv\left.\frac{\partial F_{\mathrm{harm}}}{\partial\eta_{\alpha\beta}}\right|_{T_0,\mathbf{R}_l} =\tfrac{1}{2}\sum\frac{\partial V_{l_1l_2}{}^{\alpha_1\alpha_2}}{\partial\eta_{\alpha\beta}}C(T)_{l_1-l_2}{}^{\alpha_1\alpha_2}. \tag{5.11}$$

The derivative on the right side can be read from (5.1) and (5.3) and is

$$\frac{\partial V_{l_1l_2}{}^{\alpha_1\alpha_2}}{\partial\eta_{\alpha\beta}}=\sum_{l_3} V_{l_1l_2l_3}{}^{\alpha_1\alpha_2\alpha}R_{l_3-l_2}{}^{\beta}. \tag{5.12}$$

Since, for high temperatures, $\mathbf{C}(T)_l\propto T$,

$$F_{0\alpha\beta;T}=(M/2T)\sum V_{l_10l_3}{}^{\alpha_1\alpha_2\alpha}R_{l_3}{}^{\beta}C_{l_1}{}^{\alpha_1\alpha_2}. \tag{5.13}$$

In Eqs. (5.11)–(5.13) the sums are over repeated indices. The sum in (5.13) is determined by the range of V_3 and is much more convenient than the $\mathbf{q}$-space form in Ref. 15.

VI. ANHARMONIC CONTRIBUTIONS TO THE FREE ENERGY

The Helmholtz free energy is given by

$$F=-k_BT\ln(\mathrm{Tr}e^{-\beta H}) \tag{6.1}$$

$$=F_{\mathrm{harm}}-k_BT\ln\langle e^{-\beta V_A}\rangle^0, \tag{6.2}$$

where the second equality involves neglect of quantum effects in the anharmonic terms. The linked-cluster theorem [Sec. III above Eq. (2.22)] gives

$$F=F_{\mathrm{harm}}-k_BT\langle e^{-\beta V_A}-1\rangle_C{}^0, \tag{6.3}$$

of which the terms proportional to V_4 and $V_3{}^2$ are represented in Figs. 4(a) and 4(b), respectively, and are (sums over repeated indices)

$$F_4=\tfrac{1}{8}N\sum V_{l_1l_2l_30}{}^{\alpha_1\alpha_2\alpha_3\alpha_4}C_{l_1-l_2}{}^{\alpha_1\alpha_2}C_{l_3}{}^{\alpha_3\alpha_4} \tag{6.4}$$

[15] J. C. P. Miller, Math. Comp. (Formerly: MTAC) 14, 130 (1960).

and

$$F_3=-\frac{N}{12k_BT}\sum V_{l_1l_20}{}^{\alpha_1\alpha_2\alpha_3}V_{l_4l_50}{}^{\alpha_4\alpha_5\alpha_6}\times C_{l_1-l_4+l_3}{}^{\alpha_1\alpha_4}C_{l_2-l_5+l_3}{}^{\alpha_2\alpha_5}C_{l_3}{}^{\alpha_3\alpha_6}. \quad (6.5)$$

The range of the sums for F_4 is determined by the CP, while in F_3 the arguments used in Sec. IV show that the l_3 summand is $O(\rho_{l_3}{}^{-9})$ in the asymptotic region, so that it converges well. Note that the structures of F_4 and M_1 are the same if $\mathbf{C}_{l_1-l_2}$ is replaced by $\mathbf{B}_{l_1-l_2}$ in the latter, and likewise for F_3 and M_2 if $\mathbf{C}_{l_3}$ is replaced by $\mathbf{B}_{l_3}$.

VII. NUMERICAL CALCULATIONS AND RESULTS

Calculation of $C_l{}^{\alpha\beta}$ and $B_l{}^{\alpha\beta}$

In this section we discuss the evaluation of the singular Brillouin-zone integrals, (3.12) for $\mathbf{C}_l$ and (4.18) for $\mathbf{B}_l$, and give numerical results. Values of $\mathbf{B}_l$ for larger ρ_l are not needed and values of $\mathbf{C}_l$ for larger ρ_l are calculated using the asymptotic forms. The latter values of $\mathbf{C}_l$ are not needed in the calculation of M_1, M_3, and M_4, while in the calculation of M_2, neglect of terms which contain a $\mathbf{C}_l$ with $\rho_l>6$ leads to an error of about 4% as compared to an error of about 1% when not neglected. If one were to try to evaluate the M_1 and M_2 sums without evaluating $\mathbf{B}_l$ in reciprocal space, the contributions of $\mathbf{C}_l$ for $\rho_l>6$ would be significant. The slow convergence of this latter method is mainly in the parts giving the propagation from the place of perturbation (V vertices) to the origin, as shown in Figs. 3(b) and 3(d). The rearrangements [Eqs. (4.19) and (4.20)] which introduce $\mathbf{B}_l$, together with the $\mathbf{q}$ form of $\mathbf{B}_l$ [Eq. (4.18)], in effect describe this propagation in the phonon representation. The remaining direct-space sums converge much more quickly.

The calculation of $\mathbf{C}_l$ and $\mathbf{B}_l$ are discussed together, since their integrands both have the q^{-2} singularity which gives rise to the principal difficulty in their numerical integration. One method of treating this singularity is to ignore it, that is, to use a numerical integration formula in which none of the evaluation points coincides with the singular point. Another method is to substract off the singular part and integrate it separately. (The dimensionless variables introduced in Sec. III will be used.) For $\mathbf{C}_l$ the unbounded singular part is the term $\mathbf{f}_{-2}(\hat{k})/k^2$ in Eq. (3.13). We write

$$\mathbf{C}_l=\frac{k_BT}{4M}\Big[\int_{\mathfrak{R}_0}d^3k\left(\mathbf{D}^{-1}(\mathbf{k})-\frac{\mathbf{f}_{-2}(\hat{k})}{k^2}\right)\cos(\pi\mathbf{k}\cdot\boldsymbol{\varrho}_l)+\int_{\mathrm{BZ}-\mathfrak{R}_0}d^3k\,\mathbf{D}^{-1}(\mathbf{k})\cos(\pi\mathbf{k}\cdot\boldsymbol{\varrho}_l)\Big]+\frac{k_BT}{4M}\int d\Omega\,\mathbf{f}_{-2}(\hat{k})\frac{\sin[\pi\mathbf{K}(\hat{k})\cdot\boldsymbol{\varrho}_l]}{\pi\hat{k}\cdot\boldsymbol{\varrho}_l}, \quad (7.1)$$

where $\mathfrak{R}_0$ is a region of the Brillouin zone about the origin, $\mathbf{K}$ is a vector from the origin to the point on the boundary surface of $\mathfrak{R}_0$ in the direction $\hat{k}$, and $d\Omega$ is the element of solid angle. In the last term on the right side in Eq. (7.1) the radial k integration has been done. The function $\mathbf{D}^{-1}-\mathbf{f}_{-2}/k^2$ is now bounded, although still nondifferentiable at the origin. This singularity presents no difficulty analytically. The method of subtracting the singularity is used to compute the values used in subsequent calculations, since it was found to be more accurate ($\leq 0.2\%$ error as compared to $\geq 2\%$ error when the singularity was neglected). The additional computer time required for the two-dimensional integral in Eq. (7.1) is small.

The corresponding expression for $\mathbf{B}_l$ is

$$\mathbf{B}_l=\frac{(k_BT)^2}{4M^2}\Big[\int_{\mathfrak{R}_0}d^3k\left((\mathbf{D}^{-1})^2-\frac{(\mathbf{f}_{-2})^2}{k^4}\right)[1-\cos(\pi\mathbf{k}\cdot\boldsymbol{\varrho}_l)]+\int_{\mathrm{BZ}-\mathfrak{R}_0}d^3k\,(\mathbf{D}^{-1})^2[1-\cos(\pi\mathbf{k}\cdot\boldsymbol{\varrho}_l)]\Big]+\frac{(k_BT)^2}{4M^2}\int d\Omega\,(\mathbf{f}_{-2})^2\left(\frac{\cos(\pi\mathbf{K}\cdot\boldsymbol{\varrho}_l)-1}{K}+\frac{\pi\mathbf{K}\cdot\boldsymbol{\varrho}_l}{K}\int_0^{\pi\mathbf{K}\cdot\boldsymbol{\rho}_l}\frac{\sin x}{x}dx\right), \quad (7.2)$$

where $(\mathbf{D}^{-1})^2$ and $\mathbf{f}_{-2}{}^2$ are matrix products. Neglect of this singularity gives less accurate results than those obtained for $\mathbf{C}_l$ because of the more complex angular variation near $\mathbf{k}=0$. The asymptotic behavior $\mathbf{B}_l\sim\rho_l$ is determined by the $\mathbf{K}\cdot\boldsymbol{\varrho}_l$ factor on the last line of (7.2).

The Brillouin-zone volume integrations were done by subdividing $\mathbf{q}$ (or $\mathbf{k}$) space into cubic integration cells and using in each cell a 27-point numerical integration formula due to Miller,[16] which is suitable for three-dimensional integrals. The vertices of the cubic grid used were obtained by dividing the distance from the origin to the centers of the square faces, $\mathbf{k}=(1,0,0)$ etc., into eight equal parts. Thus the origin is the vertex of eight cells which comprise the region $\mathfrak{R}_0$ in (7.1) and (7.2) where the singularity is subtracted out, while the square faces of the zone lie in faces of the cells. The hexagonal faces of the zone can intersect cells but, because the integrands are periodic, it is sufficient to integrate over all cells whose centers are in the interior of the zone. That part of a cell which protrudes through a hexagonal face corresponds to an equivalent interior volume at the opposite hexagonal face of a cell whose center is outside the zone. A factor $\frac{1}{2}$ is needed for cells whose center lies on a hexagonal face.

If the integrand has cubic symmetry also, then a further reduction is achieved by integrating only over

[16] A. A. Maradudin, Phys. Status Solidi 2, 1493 (1962).

each cell which intersects the sector S_1 defined by $q_1 \geq q_2 \geq q_3$ and multiplying the contribution of that cell by $48/\mu$, where μ is the number of sectors $S_1, \cdots, S_{48}$ which it intersects. The factor $1/\mu$ comes from the fact that, if this procedure were applied to all 48 sectors and the results added up, the contribution of each region of cell i would be counted μ_i times. The volume integrands in (7.1) and (7.2) are of the form $\mathbf{F}(\mathbf{k}) \times \cos(\pi \mathbf{k} \cdot \boldsymbol{\varrho}_l)$, where $\mathbf{F}$ carries tensor indices. Because of the tensor indices and the $\boldsymbol{\varrho}_l$, each component does not have cubic symmetry. It is possible, however, to introduce a function of cubic symmetry which permits evaluating the integral by using only the cells which intersect S_1. We make use of the symmetry property which may be verified for all of the tensor functions that we encounter here, namely,

$$\mathbf{F}(\mathcal{T}\mathbf{k}) = (T\mathbf{F})(\mathbf{k}), \tag{7.3a}$$

$$\boldsymbol{\phi}(\mathcal{T}\boldsymbol{\varrho}_l) = (T\boldsymbol{\phi})(\boldsymbol{\varrho}_l), \tag{7.3b}$$

where $T\mathbf{F}$ or $T\boldsymbol{\phi}$ denotes the matrix transformation on all of the tensor indices and the right-hand members are to be evaluated for the original arguments. Equations (2.13c) and (3.3) are examples of (7.3b). Now

$$\begin{aligned}\int_{\mathrm{BZ}} d^3k\, \mathbf{F}(\mathbf{k}) \cos(\pi \mathbf{k} \cdot \boldsymbol{\varrho}_l) &= \sum_{t=1}^{48} \int_{S_t} d^3k\, \mathbf{F}(\mathbf{k}) \cos(\pi \mathbf{k} \cdot \boldsymbol{\varrho}_l) \\ &= \int_{S_1} d^3k \sum_{t=1}^{48} \mathbf{F}(\mathcal{T}_t \mathbf{k}) \cos[\pi (\mathcal{T}_t \mathbf{k}) \cdot \boldsymbol{\varrho}_l] \\ &\equiv \int_{S_1} d^3k\, \mathbf{F}'(\mathbf{k}),\end{aligned}$$

where $\mathcal{T}_t$ is the transformation which takes S_1 into S_t. Because t runs over the entire cubic group (48 elements), it is easily verified that $\mathbf{F}'(\mathcal{T}\mathbf{k}) = \mathbf{F}'(\mathbf{k})$, which means that each component of $\mathbf{F}'$ can be extended from S_1 throughout the Brillouin zone as a symmetric function of $\mathbf{k}$. The final integration formula for a second-rank tensor which was used is

$$\begin{aligned}\int_{\mathrm{BZ}} d^3k\, F^{\alpha\beta}(\mathbf{k}) \cos(\pi \mathbf{k} \cdot \boldsymbol{\varrho}_l) &= 2 \sum_{t=1}^{24} \sum_{\alpha',\beta'} T_{t\alpha\alpha'} T_{t\beta\beta'} \sum_{\substack{\text{cells } i \text{ which} \\ \text{intersect } S_1}} \frac{1}{\mu^i} \int_i d^3k \\ &\quad \times F^{\alpha',\beta'}(\mathbf{k}) \cos(\pi \mathbf{k} \cdot \mathcal{T}_t^{-1} \boldsymbol{\varrho}_l),\end{aligned} \tag{7.4}$$

where the first sum is restricted to proper transformations. For the mesh size used there are 60 cells i.

The singularity in (7.1) and (7.2) was subtracted out in the volume $\mathcal{R}_0$ of the eight cubes about the origin. The remaining two-dimensional solid-angle integral was converted to an integral over the surface of $\mathcal{R}_0$. The surface was subdivided into a square mesh by dividing the distance from the center of a square face to the center of an edge into eight equal parts. Again only the cells intersecting 1/48 of the integration region need be used. There are 55 for the mesh used. In each cell a nine-point integration formula due to Miller[16] was used.

For each value of $\boldsymbol{\varrho}_l$ the computation time on an IBM 7040 was about 2 min for the volume integral and $\frac{1}{2}$ min for the surface integral. The volume integration was tested in several ways. For the integrable functions, $f(\mathbf{k}) = 1$, $\cos(\pi \mathbf{k} \cdot \boldsymbol{\varrho})$, $\cos^2(\pi \mathbf{k} \cdot \boldsymbol{\varrho})$, where $\boldsymbol{\varrho} = (4,4,0)$, the mesh used gave agreement to six decimal places. A $\frac{1}{3}$ reduction in the linear dimension of the integration mesh made a 0.002% further change in the value of $\mathbf{C}_l^{11}$ for $\boldsymbol{\varrho}_l = (6,0,0)$ calculated by the singularity subtraction method of Eqs. (7.1) and (7.2). In Miller's integration formula none of the points is at the cube vertices, so that (3.12) and (4.18) for $\mathbf{C}_l$ and $\mathbf{B}_l$, respectively, can be used directly by ignoring the singularity. For the mesh size used C_l^{11} was 2% too large for $\boldsymbol{\varrho}_l = (6,0,0)$ and the mesh refinement did not reduce the error much, presumably because the integration points move nearer to the singularity. Neglect of the singularity is more serious for $\mathbf{B}_l$ because of the more complex angular variation near $\mathbf{k} = 0$.

About 95% of the contribution to C_l^{11} for $\boldsymbol{\varrho}_l = (6,0,0)$ comes from the region $\mathcal{R}_0$, where the integrand is varying more rapidly than elsewhere in the Brillouin zone, and the principal source of error is the integration in (7.1) over the surface of $\mathcal{R}_0$ because of the rapid angular variation. For the smooth function $f(\mathbf{k}) = 1$ even a much coarser surface mesh than the one used gives the integral to seven decimals. To test the rapid angular variation, the integral

$$\frac{1}{2}\left(\frac{\pi}{a}\right)^{1/2} \int d\Omega\, e^{-(\pi\rho\cos\theta)^2/4\alpha} = \frac{2}{\rho} \operatorname{erf} \frac{\pi\rho}{2\alpha^{1/2}}$$

was done for $\rho = 6$, $\alpha = \frac{1}{6}$. For the mesh used the value was 1.048305 as compared with the correct value of 1.047198, a difference of 0.1%. Reducing the mesh dimension by two gave agreement to 0.002%. Errors of 2 or 3% in each $\mathbf{C}_l$ or $\mathbf{B}_l$ could lead to serious errors in M_i because of the subtractions and multiplications involved [see Eqs. (7.9) to (7.12)]. The tests above show that much smaller errors are made in the integrations used and, since even these errors are for large $\boldsymbol{\varrho}_l$, they are negligible compared with truncation errors in the M_i sums.

The calculations were done with two sets of CP for copper. The first is that of Lehman, Wolfram, and DeWames,[17] and is based on a third-neighbor central-force model. The CP were found by fitting to x-ray–determined phonon dispersion curves and to elastic constants, both at 300°K. The second set was given by

[17] G. W. Lehman, T. Wolfram, and R. E. DeWames, Phys. Rev. 128, 1593 (1962). The CP in Table III of this reference are incorrect and are corrected in the errata of Phys. Rev. 130, 2598 (1963). The corrected values are used in Ref. 24.

Sinha,[18] who fitted a sixth-neighbor tensor-force model to neutron dispersion curves and elastic constants at 300°K. The CP are listed in Table I and the values of $\mathbf{C}/a^2$ ($a=3.610\times10^{-8}$ cm) are shown in Table II. The values of $\mathbf{C}$ obtained from Lehman's model are somewhat larger than those obtained from Sinha's model. Table III gives $\mathbf{B}_l$ for $\varrho_l\leq 6$. The values obtained for $\mathbf{B}_l$ using Sinha's CP are generally larger than those obtained using Lehman's CP, although the former give smaller values for $\mathbf{C}_l$.

Test of the Asymptotic Expansion for $C_l^{\alpha\beta}$

The integrals (3.18) and (3.19) for the first two terms of the asymptotic expansion of $\mathbf{C}_l$ can be reduced to one-dimensional form because of the δ functions. The integration variables used in Eq. (3.18) have the k_3' axis along ϱ_l. Transforming back to the original variables $\mathbf{k}$ and carrying out the θ integration leads to

$$\mathbf{C}^{(1)}(\hat{\rho})=\frac{k_BT}{4M}\int d\Omega\,\mathbf{f}_{-2}(\mu,\varphi)\delta(\hat{k}\cdot\hat{\rho})$$

$$=\frac{k_BT}{2M}\xi_3\int_0^{\pi}d\varphi\,\frac{\mathbf{f}_{-2}(\mu_0(\varphi),\varphi)}{(\xi_1\cos\varphi+\xi_2\sin\varphi)^2+\xi_3^2},\quad(7.5)$$

where $\mu=\cos\theta$, $\mu_0=\cos\theta_0(\varphi)$, $\xi_i=\rho_i/\rho$, and

$$\theta_0(\varphi)=-\tan^{-1}[\rho_3/(\rho_1\cos\varphi+\rho_2\sin\varphi)].\quad(7.6)$$

In Eq. (7.5) use was made of the property that, if $g(x)$ has only simple zeros at $x=x_n$,

$$\delta(g(x))=\sum_n\frac{\delta(x-x_n)}{|(dg/dx)_{x=x_n}|}.$$

TABLE I. Parameters of the potentials used. The harmonic CP are taken from Lehman, Wolfram, and DeWames[a] and from Sinha,[b] both sets essentially from phonon data at 300°K. The anharmonic CP are assumed to be determined by the repulsive Born-Mayer pair potential. Four combinations, models I–IV, are used in the calculations of anharmonic effects.

Harmonic CP (dyn/cm)

ϱ_l	$\alpha\beta$	$-V^{\alpha\beta}$ [b]	$-V^{\alpha\beta}$ [a]	ϱ_l	$\alpha\beta$	$-V^{\alpha\beta}$ [b]
110	11	11 240	13 478	220	11	267
	33	−105	−1215		33	−32
	12	11 250	14 982		12	−36
200	11	−227	18	310	11	−110
	22	105	−48		22	−203
211	11	1122	507		33	37
	22	35	239		12	18
	23	363	159	222	11	−157
	12	725	378		12	−58

Born-Mayer parameters, $\varphi_{\text{rep}}=A\exp[-B(r-R_{nn})/R_{nn}]$

	1 Shear moduli[c]	2 Pressure dependence of shear moduli[c]	3 Cohesive energy, lattice parameter, compressibility[d]
A (eV)	0.0408	0.1081	0.0958
B	16.6	11.75	13.34

Models used for anharmonic calculations

I	Harmonic CP[a] and A_1, B_1
II	Harmonic CP[a] and A_2, B_2
III	Harmonic CP[a] and A_3, B_3
IV	Harmonic CP[b] and A_3, B_3

[a] Reference 17. [b] Reference 18. [c] Reference 20. [d] Reference 21.

TABLE II. Pair-displacement correlation functions $C_l^{\alpha\beta}$ for copper ($T=\Theta=315$°K). The units are $10^{-4}a^2=1.303\times10^{-19}$ cm^2, where $a=3.610\times10^{-8}$ cm is the cubic lattice constant. Columns marked "a" are based on the CP of Lehman, Wolfram, and DeWames[a] and those marked "b" are based on the CP of Sinha.[b] Not all of the latter values are given.

	Component								
ϱ_l	11[a]	11[b]	22[a]	22[b]	33[a]	12[a]	12[b]	23[a]	13[a]
000	5.5878	5.4688	5.5878	5.4688	5.5878	0.0	0.0	0.0	0.0
110	1.7289	1.7659	1.7289	1.7659	1.4206	0.5261	0.5879	0.0	0.0
200	0.9815	0.9468	1.0249	1.0221	1.0249	0.0	0.0	0.0	0.0
211	1.0101	1.0166	0.8991	0.9257	0.8991	0.2239	0.2222	0.1381	0.2239
220	0.8942	0.9537	0.8942	0.9537	0.7088	0.3043	0.3394	0.0	0.0
310	0.6706	0.6654	0.6866	0.6973	0.6394	0.1148	0.1097	0.0	0.0
222	0.6906	0.7031	0.6906	0.7031	0.6906	0.1877	0.1861	0.1877	0.1877
321	0.6634	0.6813	0.6348	0.6551	0.5583	0.1917	0.1996	0.0882	0.1049
400	0.4914	0.4894	0.5202	0.5321	0.5202	0.0	0.0	0.0	0.0
330	0.5918	0.6251	0.5918	0.6251	0.4567	0.2015	0.2250	0.0	0.0
411	0.5023	0.5029	0.4976	0.5115	0.4976	0.0654	0.0652	0.0302	0.0654
420	0.5065	0.5090	0.5099	0.5238	0.4437	0.1233	0.1246	0.0	0.0
332	0.5317	0.5440	0.5317	0.5440	0.4819	0.1659	0.1696	0.1248	0.1248
422	0.5024	0.5150	0.4577	0.4719	0.4577	0.1172	0.1219	0.0823	0.1172
431	0.4869	0.5025	0.4776	0.4949	0.3941	0.1520	0.1614	0.0535	0.0576
510	0.3950	0.3946	0.4163	0.4276	0.4053	0.0414	0.0418	0.0	0.0
521	0.4038	0.4065	0.4028	0.4146	0.3753	0.0811	0.0826	0.0297	0.0416
440	0.4422	0.4626	0.4422	0.4626	0.3373	0.1499	0.1645	0.0	0.0
530	0.4024	0.4083	0.4022	0.4152	0.3345	0.1119	0.1160	0.0	0.0
433	0.4364	0.4471	0.4098	0.4212	0.4098	0.1228	0.1265	0.1049	0.1228
442	0.4201	0.4325	0.4201	0.4325	0.3571	0.1372	0.1434	0.0816	0.0816
600	0.3255	0.3249	0.3495	0.3595	0.3495	0.0	0.0	0.0	0.0

[a] Reference 17. [b] Reference 18.

[18] S. K. Sinha, Phys. Rev. 143, 422 (1966).

TABLE III. Values of the function $B_l^{\alpha\beta}$ of Eq. (4.18), for copper. Units are $10^{-6}a^4=1.698\times10^{-36}$ cm^4. All the calculated values for the coupling parameters of Lehman *et al.*[a] are shown and only some of the values for the coupling parameters of Sinha.[b] ($T=\Theta$.)

	Component								
ϱ_l	11[a]	11[b]	22[a]	22[b]	33[a]	12[a]	12[b]	23[a]	13[a]
000	0.0	0.0	0.0	0.0	0.0	0.0	0.0	0.0	0.0
110	0.2809	0.2814	0.2809	0.2814	0.2982	−0.0934	−0.1012	0.0	0.0
200	0.4532	0.4700	0.4287	0.4345	0.4287	0.0	0.0	0.0	0.0
211	0.5193	0.5322	0.5203	0.5268	0.5203	−0.1058	−0.1121	−0.0582	−0.1058
220	0.5939	0.6039	0.5939	0.6039	0.6175	−0.1818	−0.1971	0.0	0.0
310	0.7134	0.7420	0.6782	0.6930	0.6887	−0.1142	−0.1215	0.0	0.0
222	0.7351	0.7551	0.7351	0.7551	0.7351	−0.1588	−0.1694	−0.1588	−0.1588
321	0.8063	0.8347	0.7955	0.8171	0.8143	−0.2063	−0.2228	−0.0790	−0.1077
400	0.9326	0.9780	0.8702	0.8938	0.8702	0.0	0.0	0.0	0.0
330	0.9053	0.9353	0.9053	0.9353	0.9393	−0.2712	−0.2965	0.0	0.0
411	0.9643	1.0104	0.9215	0.9479	0.9215	−0.1152	−0.1243	−0.0364	−0.1152
420	0.9980	1.0448	0.9586	0.9893	0.9855	−0.2209	−0.2393	0.0	0.0
332	0.9992	1.0369	0.9992	1.0369	1.0115	−0.2577	−0.2791	−0.1815	−0.1815
422	1.0672	1.1153	1.0574	1.0932	1.0574	−0.2142	−0.2327	−0.1233	−0.2142
431	1.1049	1.1537	1.0889	1.1299	1.1243	−0.3022	−0.3298	−0.0876	−0.1075
510	1.1857	1.2511	1.1094	1.1472	1.1162	−0.1167	−0.1269	0.0	0.0
521	1.2373	1.3040	1.1849	1.2287	1.2021	−0.2256	−0.2459	−0.0569	−0.1148
440	1.2156	1.2682	1.2156	1.2682	1.2607	−0.3619	−0.3971	0.0	0.0
530	1.2929	1.3609	1.2516	1.3021	1.2945	−0.3222	−0.3521	0.0	0.0
433	1.2480	1.3048	1.2513	1.3025	1.2513	−0.2834	−0.3087	−0.2250	−0.2834
442	1.2847	1.3427	1.2847	1.3427	1.3116	−0.3530	−0.3858	−0.1915	−0.1915
600	1.4140	1.5003	1.3126	1.3626	1.3126	0.0	0.0	0.0	0.0

[a] Reference 17. [b] Reference 18.

Equation (7.5) is not valid for $\xi_3=0$ but, through use of the cubic symmetry relations, $\mathbf{C}^{(1)}(\hat{\rho})$ can be found by considering another direction. Inversion symmetry of $\mathbf{f}_{-2}$ reduces the limits of integration to the range 0 to π.

Similarly, we get

$$\mathbf{C}^{(2)}(\hat{\rho})=-\frac{k_BT}{4M\pi^2}\int d\Omega\,(\Theta\mathbf{f}_0(\mu,\varphi))\delta(\hat{k}\cdot\hat{\rho})$$

$$=-\frac{k_BT}{2M\pi^2}\xi_3\int_0^{\pi}d\varphi\,\frac{(\Theta\mathbf{f}_0(\mu,\varphi))\,|_{\theta=\theta_0}}{(\xi_1\cos\varphi+\xi_2\sin\varphi)^2+\xi_3^2}. \quad (7.7)$$

The operator Θ is $\partial^2/\partial\mu'^2$ expressed in terms of the unprimed coordinates. These integrals were evaluated by means of the 80-point Gauss formula.[19]

The angular variation of $\mathbf{C}^{(1)}$ and $\mathbf{C}^{(2)}$ is shown in Table IV. Note that $\mathbf{C}^{(2)}$ varies much more rapidly than does $\mathbf{C}^{(1)}$ and that it may also be larger, for example, especially in the [111] direction. Tables V and VI compare the first term and the first two terms of the asymptotic expansion (3.17) with the values of $\mathbf{C}_l$ calculated from (3.12) and (7.1) for the 11 and 12 components, respectively. With few exceptions, for ϱ_l near zero, as might be expected, and for ϱ_l in the [110] direction, including the second term $\propto\rho^{-3}$ improves agreement. Reference to Table IV show that the largest values of $C^{(2)}$ have opposite sign to $C^{(1)}$. If the asymptotic series were alternating, then

$$\rho_l^{-1}\mathbf{C}^{(1)}(\hat{\rho}_l)+\tfrac{1}{2}\rho_l^{-3}\mathbf{C}^{(2)}(\varrho_l) \quad (7.8)$$

would be a better second approximation to $\mathbf{C}_l$ than the first two terms of (3.17). The last three columns in Tables V and VI show the percentage deviations of the first and second approximations of (3.17) and of (7.8), respectively, from the directly integrated values of $C_l^{\alpha\beta}$. Use of (7.8) improves agreement in the [110]

TABLE IV. Angular dependence of the first two terms of the asymptotic expansion (3.17) of $\mathbf{C}_l$. Units are 10^{-19} cm^2 [$=(0.767\times10^{-4})a^2$]. The values are for $T=315$°K and the second and third columns would be proportional to T. The CP of Ref. 17 were used.

ϱ_l	$C^{(1)}(\hat{\rho}_l)^{11}$	$C^{(2)}(\hat{\rho}_l)^{11}$	$C^{(2)11}/C^{(1)11}$	$C^{(1)}(\hat{\rho}_l)^{12}$	$C^{(2)}(\hat{\rho}_l)^{12}$	$C^{(2)12}/C^{(1)12}$
400	2.5350	0.3294	0.1299	0.0	0.0	...
410	2.6443	0.5544	0.2096	0.3373	0.2962	0.8780
420	2.9174	1.0956	0.3755	0.6986	0.9009	1.2896
430	3.1781	0.2347	0.0738	1.0024	0.2189	0.2184
440	3.2555	−0.7144	−0.2194	1.1089	−1.0425	−0.9401
441	3.2786	−0.9249	−0.2821	1.1124	−1.2175	−1.0944
442	3.3259	−1.8351	−0.5517	1.1123	−1.8675	−1.6788
443	3.3460	−3.3619	−1.0047	1.0834	−2.8898	−2.6672
444	3.3014	−3.8237	−1.1609	1.0072	−3.2675	−3.2440
433	3.3819	−2.6396	−0.7805	0.9828	−1.8712	−1.9039
422	3.1726	1.2040	0.3795	0.7368	0.5584	0.7579
411	2.7452	0.8289	0.3019	0.3493	0.2955	0.8459

[19] M. Abramowitz and I. A. Stegun, *Handbook of Mathematical Functions* (Dover Publications, Inc., New York, 1965), p. 918.

TABLE V. Comparison of the values of C_l^{11} for $T=315°K$ calculated as a Brillouin-zone integral (3.12) [or (7.1)] with the values calculated from the asymptotic expansion (3.17). Units are 10^{-19} cm^2. The CP are taken from Ref. 17. The last three columns are the percentage deviations (PD) of the first term of (3.17) and the first two terms of (3.17) and of (7.8) from the Brillouin-zone integral respectively.

ρ_l	(3.17), one term	(3.17), two terms	BZ integral (3.12)	PD_1	PD_2	PD_3
200	1.2675	1.3087	1.2791	−0.9084	2.3117	−0.7016
220	1.1510	1.1194	1.1653	−1.2254	−3.9355	−2.5805
222	0.9530	0.8608	0.9000	5.8931	−4.3516	0.7707
400	0.6338	0.6389	0.6404	−1.0386	−0.2347	−0.6366
420	0.6524	0.6646	0.6601	−1.1736	0.6820	−0.2458
422	0.6476	0.6579	0.6548	−1.0899	0.4742	−0.3078
440	0.5755	0.5716	0.5762	−0.1262	−0.8110	−0.4686
442	0.5543	0.5458	0.5475	1.2457	−0.3061	0.4698
600	0.4225	0.4240	0.4242	−0.3951	−0.0354	−0.2152
620	0.4306	0.4335	0.4333	−0.6169	0.0563	−0.2803
622	0.4350	0.4391	0.4385	−0.8062	0.1345	−0.3358
444	0.4765	0.4650	0.4675	1.9327	−0.5328	0.6999
640	0.4308	0.4329	0.4324	−0.3758	0.0994	−0.1382
642	0.4274	0.4291	0.4288	−0.3165	0.0721	−0.1222
800	0.3169	0.3175	0.3175	−0.2050	−0.0022	−0.1036
644	0.4065	0.4044	0.4041	0.5877	0.0624	0.3250
820	0.3207	0.3217	0.3217	−0.3152	−0.0078	−0.1615
660	0.3837	0.3825	0.3834	0.0837	−0.2212	−0.0687
822	0.3235	0.3249	0.3249	−0.4149	0.0028	−0.2061
662	0.3778	0.3761	0.3766	0.3253	−0.1269	0.0992
840	0.3262	0.3277	0.3275	−0.4146	0.0528	−0.1809
842	0.3266	0.3283	0.3282	−0.4641	0.0506	−0.2068
664	0.3566	0.3532	0.3536	0.8709	−0.1109	0.3800
844	0.3238	0.3251	0.3249	−0.3370	0.0569	−0.1400
860	0.3178	0.3180	0.3181	−0.0965	−0.0226	−0.0596
1000	0.2535	0.2538	0.2541	−0.2181	−0.0882	−0.1531

direction. The asymptotic expansion works surprisingly well, the first term alone agreeing to within 6% even for small ρ_l and the values from (7.8) to within 3%. Note, for example, that in the [100] direction agreement improves as ρ_l increases out to $\rho_l=(8,0,0)$ and worsens at $\rho_l=(10,0,0)$. This indicates that the volume integrations [in (7.1)] are becoming inaccurate because of the rapid oscillation of $\cos(\pi\mathbf{k}\cdot\rho_l)$.

TABLE VI. Comparison of the values of C_l^{12} for $T=315°K$ calculated as a Brillouin-zone integral (3.12) [or (7.1)] with the values calculated from the asymptotic expansion (3.17). Units are 10^{-19} cm^2. The CP are taken from Ref. 17. The last three columns are the percentage deviations (PD) of the first term of (3.17) and the first two terms of (3.17) and of (7.8) from the Brillouin-zone integral, respectively.

ρ_l	(3.17), one term	(3.17), two terms	BZ integral (3.12)	PD_1	PD_2	PD_3
200	0.0	0.0	0.0	...	...	...
220	0.3921	0.3460	0.3966	−0.3881	−4.3421	−2.3651
222	0.2908	0.2122	0.2446	5.1335	−3.6003	0.7666
400	0.0	0.0	0.0	...	...	...
420	0.1562	0.1663	0.1607	−0.6805	0.8455	0.0825
422	0.1504	0.1552	0.1527	−0.3476	0.3778	0.0151
440	0.1960	0.1903	0.1954	0.1085	−0.8911	−0.3913
442	0.1854	0.1768	0.1788	1.2009	−0.3783	0.4113
600	0.0	0.0	0.0	...	...	...
620	0.0721	0.0740	0.0738	−0.3837	0.0599	−0.1619
622	0.0723	0.0740	0.0738	−0.3360	0.0450	−0.1455
444	0.1454	0.1356	0.1375	1.6762	−0.4257	0.6253
640	0.1273	0.1292	0.1284	−0.2639	0.1792	−0.0423
642	0.1248	0.1258	0.1252	−0.0917	0.1227	0.0155
800	0.0	0.0	0.0	...	...	...
644	0.1125	0.1110	0.1107	0.4451	0.0698	0.2575
820	0.0409	0.0414	0.0414	−0.1644	−0.0002	−0.0823
660	0.1307	0.1290	0.1299	0.2157	−0.2296	−0.0069
822	0.0412	0.0417	0.0417	−0.1493	−0.0005	−0.0749
662	0.1278	0.1257	0.1262	0.4055	−0.1442	0.1306
840	0.0781	0.0794	0.0791	−0.3144	0.0700	−0.1222
842	0.0779	0.0790	0.0788	−0.2710	0.0597	−0.1057
664	0.1170	0.1139	0.1143	0.7801	−0.0959	0.3421
844	0.0752	0.0758	0.0756	−0.1351	0.0476	−0.0437
860	0.1002	0.1005	0.1003	−0.0311	0.0377	0.0033
1000	0.0	0.0	0.0	...	...	...

TABLE VII. Thermal expansion coefficient of copper at $T=300°K$ (in 10^{-6} $°K^{-1}$).

Experimental value[a]	1.672
Model I	2.251
Model II	1.931
Model III	2.603
Model IV	2.407

[a] I. E. Leksina and S. I. Novikova, Fiz. Tverd. Tela 5, 1094 (1963) [English transl.: Soviet Phys.—Solid State 5, 798 (1963)].

The advantage of using the asymptotic expansion for small ρ_l also is the smaller computation time. To compute $C_l^{\alpha\beta}$ took $2\frac{1}{2}$ min per point ρ_l, while to compute $C^{(1)\alpha\beta}$ and $C^{(2)\alpha\beta}$ took 2 sec and 1 min per point. respectively, on the IBM 7040.

Calculation of Anharmonic Contributions to the Debye-Waller Factor

Third- and fourth-order CP were obtained as follows. The configurational potential energy can be separated into long- and short-range parts, the long-range part due to the electronically screened interaction between ions and the short-range repulsive interaction resulting from the interpenetration of the outer shells of nearby ions. The repulsive part is usually described by the Born-Mayer *pair* potential

$$\varphi_{\rm rep}(r)=Ae^{-B[(r-R_{\rm nn})/R_{\rm nn}]},$$

where A and B are parameters, the values of which have been estimated semiempirically by serveral methods and which are rather widely scattered.[20,21] These values are shown in Table I. Our basic *assumption* is that V_3, V_4, etc., which involve higher derivatives of the potential energy than does V_2, are predominantly determined by $\varphi_{\rm rep}$. This is supported by the estimate of Mann and Seeger[20] of the relative contribution of the valence electrons and $\varphi_{\rm rep}$ to the derivatives of the total energy with respect to specific volume, namely, the valence electrons contribute 23, 6, and 0.4% to the second, third, and fourth derivatives, respectively. The anharmonic CP can then be calculated (but not V_2) as if there were central forces.

The form of the CP for central forces is given in the Appendix. When these CP are substituted into Eqs. (4.19)–(4.22), the following equations result (with sums over repeated indices);

$$M_1=-\tfrac{1}{6}\beta\kappa^2\sum v_l{}^{\alpha_1\alpha_2\alpha_3\alpha_4}(C_0-C_l)^{\alpha_3\alpha_4}B_l{}^{\alpha_1\alpha_2}, \quad (7.9)$$

$$M_2=-\tfrac{1}{12}\beta^2\kappa^2\sum v_{n_1}{}^{\alpha_1\alpha_2\alpha_3}v_{n_2}{}^{\alpha_4\alpha_5\alpha_6}\times(C_l-C_{l+n_1}-C_{l+n_2}+C_{l+n_1+n_2})^{\alpha_1\alpha_4}\times(C_l-C_{l+n_1}-C_{l+n_2}+C_{l+n_1+n_2})^{\alpha_2\alpha_5}B_l{}^{\alpha_3\alpha_6}, \quad (7.10)$$

$$\mathfrak{M}_3{}^{\alpha\beta\gamma\delta}=\frac{\beta}{24}\sum v_n{}^{\alpha_1\alpha_2\alpha_3\alpha_4}(C_l-C_{l+n})^{\alpha_1\alpha}(C_l-C_{l+n})^{\alpha_2\beta}\times(C_l-C_{l+n})^{\alpha_3\gamma}C_l{}^{\alpha_4\delta}, \quad (7.11)$$

$$\mathfrak{M}_4{}^{\alpha\beta\gamma\delta}=-\tfrac{1}{16}\beta^2\sum v_{n_1}{}^{\alpha_1\alpha_2\alpha_3}v_{n_2}{}^{\alpha_4\alpha_5\alpha_6}(C_l-C_{l+n_1})^{\alpha_1\alpha}\times(C_l-C_{l+n_1})^{\alpha_2\beta}(C_{l'}-C_{l'+n_2})^{\alpha_4\gamma}\times(C_{l'}-C_{l'+n_2})^{\alpha_5\delta}(C_{l-l'}-C_{l+l'})^{\alpha_3\alpha_6}. \quad (7.12)$$

In each of Eqs. (7.9)–(7.12) *one* of the sums over atoms, say, $\mathbf{l}=(l_1,l_2,l_3)$, can be restricted to the solid-angle sector $l_1\geq l_2\geq l_3$ by including a weight factor ν_l. This sector contains a unique representative from each atomic shell about the origin and ν_l is the number of atoms in the shell. Each atom l' in a shell is reached by some symmetry rotation $\mathcal{T}$ which takes the representative atom l into it and, by reference to (3.3) (which holds for both $\mathbf{C}_l$ and $\mathbf{B}_l$) and (A5) [or to (7.3b) for all], we see that this is equivalent to the orthogonal transformation $\mathbf{T}$ on the tensor indices while holding l fixed. In M_1 all tensor indices are contracted in pairs, giving an invariant under $\mathbf{T}$, so that the contributions for each l are the same. For M_2 the proof is similar but requires also a change in variables $n_{1,2}\rightarrow n_{1',2'}$ for each l', so that, if $\mathcal{T}l=l'$, $\mathcal{T}n=n'$.

The uncontracted indices in $\mathfrak{M}_{3,4}{}^{\alpha\beta\gamma\delta}$ modify the above argument. Consider $\mathfrak{M}_3$ (with tensor indices suppressed for the moment) and let $\mathfrak{M}_3(l')$ be the contribution in (7.11) from an atom l' in the same shell as atom l. Then

$$\mathfrak{M}_3=\sum_{l' \text{ in shell}}\mathfrak{M}_3(l').$$

Let $\mathcal{T}_{l'}$ be such that $\mathcal{T}_{l'}l=l'$. Then the procedure used above for M_2 gives readily

$$\mathfrak{M}_3(l')=T_{l'}\,\mathfrak{M}_3(l),$$

where T transforms the tensor indices. Now we use the special property of cubic symmetry that the nonzero elements have indices $\alpha\alpha\beta\beta$, $\alpha\beta\alpha\beta$, or $\alpha\alpha\alpha\alpha$ and that, for example,

$$\mathfrak{M}_3{}^{xxyy}=\mathfrak{M}_3{}^{yyzz}=\mathfrak{M}_3{}^{zzxx}.$$

Also, $T(\alpha\alpha\beta\beta)=\alpha'\alpha'\beta'\beta'$, and similar relations, so that

$$\mathfrak{M}_3(l')=\mathfrak{M}_3(l)$$

and the ν_l factor is applicable. The argument clearly applies also to the l sum in (7.12) for $\mathfrak{M}_4$.

In calculating $\mathfrak{M}_4$ it was expedient to calculate and store the component sum

$$S_l{}^{\alpha_1\alpha\beta}\equiv\sum_n\sum_{\alpha_2,\alpha_3}v_n{}^{\alpha_1\alpha_2\alpha_3}(C_l-C_{l+n})^{\alpha_2\alpha}\times(C_l-C_{l+n})^{\alpha_3\beta}, \quad (7.13)$$

in terms of which

$$\mathfrak{M}_4{}^{\alpha\beta\gamma\delta}=-\tfrac{1}{16}\beta^2\sum_l{}'\,\nu_l\sum_{l'}S_l{}^{\alpha_1\alpha\beta}S_{l'}{}^{\alpha_2\gamma\delta}\times(C_{l-l'}-C_{l+l'})^{\alpha_1\alpha_2}, \quad (7.14)$$

[20] E. Mann and A. Seeger, J. Phys. Chem. Solids 12, 314 (1967).
[21] S. S. Jaswal and L. A. Girifalco, J. Phys. Chem. Solids 28, 457 (1967).

where the prime refers to restricting l to the reference sector $l_1 \geq l_2 \geq l_3$ or, equivalently, to the sum over atomic shells.

In the machine calculations the relevant data, ϱ_l, $v_l{}^{\alpha\cdots}$, $C_l{}^{\alpha\beta}$, $S_l{}^{\alpha\beta\gamma}$, etc., were read in for l in the reference sector only. Values needed for l outside were calculated from the corresponding reference-sector values by use of the transformations

$$(Q_{l'})^{\alpha\cdots} = (T_{l'}Q)^{\alpha\cdots}. \tag{7.15}$$

Much time is saved because each $T_{l'}$ has only three nonzero elements.

The thermal expansion $\eta(T)$ is easily calculated from Eqs. (5.9) and (5.13). The value of T_0 is 300°K, since the CP in Refs. 17 and 18 were determined at this temperature. The isothermal compressibility is $B_0{}^{is} = 13.317\times10^{11}$ dyn cm^{-2}.[22] Table VII shows the calculated and experimental values of the thermal expansion coefficient. The variation among the first three models (see Table I) is due to the different Born-Mayer parameters. The difference of the last two values comes from the harmonic CP. The experimental value of the thermal expansion coefficient was used to get the change in M_0 (or $C_0{}^{11}$) from Eq. (5.6). The singularity in (5.6) was neglected, since this leads to a negligible error in the Debye-Waller factor.

Table VIII shows the various contributions to the Debye-Waller factor for the models used. There is a large cancellation of V_3 and V_4 contributions to the mean-square displacement (κ^2 terms) in the upper part of the table. As a result, the first quantum correction is comparable with the anharmonic effect at the Debye temperature. The V_3 and V_4 contributions add (negatively) in the anisotropic term $\kappa^4\Delta m_A{}^{(4)}h_1(\hat{\kappa})$ and the resultant is not very sensitive to the choice of potential. To estimate the importance of the anisotropy, consider $M_0\sim1$, or $\kappa a\sim60$ (minimum value for Bragg reflection is $\kappa a = 2\sqrt{3}\pi\sim11$). Then the anisotropic term has an amplitude about 0.4% of m_0.

The first quantum correction has been included in M_0. The second quantum correction would be about 1/60 as large. The quantum corrections to the anharmonic terms are also negligible relative to M_0. However, if they were significant, it would not be consistent to calculate them by correcting $C_l{}^{\alpha\beta}$ by using (3.5) in (3.4), because comparable terms are neglected in replacing $U(\beta)$ in (2.7) by $e^{-\beta V_A}$ (see Ref. 10).

Table IX shows a number of calculated values of the mean-square displacement, including the present work, and the values determined by x-rays by Flinn, McManus, and Rayne.[23] Only in the present work are the anharmonic contribution and the thermal expansion included. The other calculated values are just for the harmonic contribution $\langle\mathbf{u}^2\rangle^0$, based on (3.4), and include

[22] W. C. Overton, Jr., and J. Gaffney, Phys. Rev. **98**, 969 (1955).
[23] P. A. Flinn, G. M. McManus, and J. A. Rayne, Phys. Rev. **123**, 809 (1961).

TABLE VIII. Contributions to the Debye-Waller factor $f=e^{-M}$ to order V_4, $V_3{}^2$.[a]

$$M = M_0+M_1+M_2+M_3+M_4{}^{b}$$
$$M_0 = (\kappa a)^2(T/\Theta)[m_0+m_0'(T-T_0)+m_0{}^{Q}(\Theta/T)^2]$$
$$M_{1,2} = (\kappa a)^2(T/\Theta)^2 m_{1,2}, \quad m_1+m_2 \equiv m_A{}^{(2)}$$
$$M_{3,4} = (\kappa a)^4(T/\Theta)^3[\tilde{m}_{3,4}+\Delta m_{3,4}h_1(\hat{\kappa})]$$
$$\tilde{m}_3+\tilde{m}_4 \equiv \tilde{m}_A{}^{(4)}, \quad \Delta m_3+\Delta m_4 \equiv \Delta m_A{}^{(4)}, \quad h_1 = \frac{5}{2}\left(\sum_\alpha \frac{\kappa_\alpha{}^4}{\kappa^4} - \frac{3}{5}\right)$$
$$\Theta = 315°\text{K}, \quad a = 3.610\times10^{-8}\text{ cm}$$

(a) All entries to be multiplied by 10^{-4}

Model	m_0 [c]	m_0' (°K)$^{-1}$ [d]	$m_0{}^{Q}$ [e]	m_1 [f]	m_2 [g]	$m_A{}^{(2)}$
I	2.794	6.65×10^{-5}	0.078	−0.368	0.316	−0.053
II	2.794	5.42×10^{-5}	0.078	−0.197	0.294	0.098
III	2.794	7.47×10^{-5}	0.078	−0.318	0.483	0.165
IV	2.734	7.04×10^{-5}	0.078	−0.279	0.448	0.169

(b) All entries to be multiplied by 10^{-10}

Model	$\tilde{m}_3$ [h]	$\tilde{m}_4$ [h]	$\tilde{m}_A{}^{(4)}$	Δm_3 [i]	Δm_4 [i]	$\Delta m_A{}^{(4)}$
I	3.63	−4.73	−1.10	−1.75	−1.31	−3.06
II	1.94	−4.16	−2.22	−1.45	−1.28	−2.73
III	3.13	−6.99	−3.86	−1.96	−2.06	−4.02
VI	2.33	−5.01	−2.68	−1.60	−1.60	−3.20

[a] See Table I for potential models.
[b] Times on IBM 7040 for Mi, $i=1, 2, 3, 4$, were 1.5, 8.5, 3.2, and 13 min, respectively.
[c] $m_0 = C_0{}^{11}(T=\Theta)/2a^2$.
[d] $m_0' = \Delta C_0{}^{11}(T=\Theta)/2a^2$, Eq. (5.6), with $\eta \to d\eta/dT = 1.672\times10^{-5}$ (°K)$^{-1}$.
[e] $m_0{}^{Q} = \hbar^2/24k_B\Theta Ma^2$ [see Eq. (3.11)].
[f] See Eqs. (4.19) and (7.9).
[g] See Eqs. (4.20) and (7.10).
[h] $\tilde{m}_{3,4} = \frac{1}{8}[\mathfrak{M}(\Theta)_{3,4}{}^{11}+\frac{1}{2}\mathfrak{M}(\Theta)_{3,4}{}^{12}]/a^2$; see Eqs. (4.9), (4.10), (4.12), (4.15), (7.11), and (4.12).
[i] $\Delta m_{3,4} = \frac{1}{8}(\mathfrak{M}_{3,4}{}^{11}-\mathfrak{M}_{3,4}{}^{12})$.

quantum terms. It is not clear why the harmonic values obtained by us do not agree better with those of Sinha[18] and DeWames *et al.*[24] for the same CP. The differences could come about from the treatment of the singularity in (3.12) at $\mathbf{q}=0$.

At 300°K all of the calculations are consistent with the experimental value, but at 400°K it is likely that such consistency requires inclusion of the anharmonic contributions and thermal expansion.

Anharmonic Contributions to the Free Energy

Because of the similarity of F_3 and F_4 to M_1 and M_2 as mentioned at the end of Sec. VI, F_3 is obtained from (7.9) by the replacements $-\frac{1}{6}\beta\kappa^2 \to \frac{1}{8}N$, $\mathbf{B}_l \to \mathbf{C}_l$, and F_4 is obtained from (7.10) by the replacements $-\frac{1}{12}\beta^2\kappa^2 \to -N/12k_BT$, $\mathbf{B}_l \to \mathbf{C}_l$. Table X gives the calculated values of F_3, F_4, and $F_A = F_3+F_4$ for the four models. For each the net contribution is positive, although F_3 is necessarily negative. The anharmonic contribution to the specific heat at constant volume is given in this temperature range by

$$C_{V_A} = -(2/T)F_A, \tag{7.16}$$

and is negative.

[24] R. E. DeWames, T. Wolfram, and G. W. Lehman, Phys. Rev. **131**, 528 (1963).

TABLE IX. Mean-square atomic displacements in copper (in 10^{-18} cm^2).

	300°K			400°K			
	$\langle u^2\rangle^0$	Anharmonic contribution	$\langle u^2\rangle$	$\langle u^2\rangle^0$	Anharmonic contribution	Thermal expansion	$\langle u^2\rangle$
Present work[a] I	2.145	−0.043	2.102	2.843	−0.077	0.066	2.832
II	2.145	+0.069	2.214	2.843	+0.123	0.053	3.019
III	2.145	0.117	2.262	2.843	0.208	0.074	3.125
IV	2.100	0.120	2.220	2.762	0.214	0.070	3.046
Sinha[b]	2.073			2.725			
Lehman *et al.*[c,d]	2.152			2.833			
White[e]	2.004			2.635			
Jacobsen[f]	2.260			2.981			
Leighton[g]	2.073			2.734			
	Experiment[h] 2.142±0.138			3.100±0.247			
	$10^3\langle u^2\rangle/a^2=1.644\pm0.105$			$10^3\langle u^2\rangle/a^2=2.379\pm0.189$			

[a] Includes first quantum correction, 0.064 for $T=300$°K, 0.047 for $T=400$°K. All the other calculations use the general form (3.4) for C^0[11].
[b] Reference 18.
[c] Remaining values d–g were calculated by DeWames, Wolfram, and Lehman (Ref. 24), using the CP taken from the designated references.
[d] Reference. 17.
[e] H. C. White, Phys. Rev. 112, 1092 (1958).
[f] E. H. Jacobsen, Phys. Rev. 97, 654 (1955).
[g] R. B. Leighton, Rev. Mod. Phys. 20, 165 (1948).
[h] Reference 23.

VIII. DISCUSSION

Although a simple correspondence is not to be expected, a comparison of the relative importance of the anharmonic contributions to the Debye-Waller factor obtained here with those calculated by Maradudin and Flinn for lead[2] is of interest. The relative individual contributions of M_1 and M_2 to $\langle\mathbf{u}^2\rangle$ at $T=\Theta$ are several times larger here (Table IX): 7 to 17% of M_0, as compared with 3 to 6% in Ref. 2. After the cancellation of M_1 with M_2 the results are comparable magnitude but of opposite sign, except for model I.

The most striking difference is in the κ^4 terms, in particular, in the anisotropic part which is the most likely observable feature of them. Referring to Table VIII, we get the ratio $\Delta m_A{}^{(4)}/m_0\sim-10^{-6}$ as compared with the value of about -10^{-9} found by Maradudin and Flinn. Consequently we think that this anisotropy should be observable in copper, at least near the melting point. The relative strengths of the cubic and quartic anharmonic coefficients are comparable in copper and lead. If $\phi^{(n)}$ denotes the nth derivative of the pair potential between nearest neighbors, then the ratios $\phi^{(2)}:a\phi^{(3)}:a^2\phi^{(4)}=1:-26:541$ for lead and $1:-35:663$ for copper, where a is the cubic lattice constant. It is possible that part of the reason for the small value of the κ^4 terms for lead is in the approximations used to simplify the M_3 and M_4 Brillouin-zone integrations. For example, there is a large cancellation in their coefficient of the anistropy function $h_1(\hat{\kappa})$, whereas Table VIII shows that the V_3 and V_4 contributions reinforce one another.

Of the potential models used here all but I, which has the "hardest" Born-Mayer repulsion, give Debye-Waller factors in Table IX which are consistent with experiment. There is little to discriminate among the other three, although Tables VII and X suggest that analysis of calorimetric as well as x-ray data may provide a basis for discrimination.

In the calculation of anharmonic contributions to the free energy we, like Wallace,[25] obtain positive values for each model and find that, for a given set of second-order CP, the shorter-range anharmonic potentials give larger contributions. What is perhaps surprising is that the values obtained for models III and IV differ so much, which indicates that these quantities are quite sensitive to small changes in the pair-displacement correlation function or phonon spectrum.

The method developed here of combining lattice sums and Brillouin-zone integrations is quite general. We have used it for third- and sixth-neighbor models for the harmonic spectrum. Noncentral third- and fourth-order CP could be handled without extra difficulty if they become available. It would be of interest to consider the longer anharmonicities which result from the Friedel oscillations of the screened ion pseudopotentials.[26]

TABLE X. Anharmonic contributions to the vibrational free energy per atom [in 10^{-15} $(T/\Theta)^2$ erg and for $a=3.610\times10^{-8}$ cm].[a]

Model	F_3	F_4	$F_A=F_3+F_4$
I	−1.171	4.593	3.422
II	−1.058	2.551	1.493
III	−1.761	4.055	2.294
VI	−1.618	3.477	1.859
$\Theta=315$°K			

[a] Time on IBM 7040 was 6 min 13 sec for F_3 and 11 sec for F_4.

APPENDIX: CP FOR CENTRAL FORCES

Suppose that V has the form

$$V=\tfrac{1}{2}\sum_{m\neq n}\varphi(r_{mn}),\quad r_{mn}=|\mathbf{r}_m-\mathbf{r}_n|. \tag{A1}$$

[25] D. C. Wallace, Phys. Rev. 131, 2046 (1963).
[26] See, for example, V. Heine and D. Weaire, Phys. Rev. 152, 603 (1966).

Using the definition (2.12) and the relation

$$\frac{\partial f(r_{mn})}{\partial r_l{}^\alpha}=(\delta_{lm}-\delta_{ln})\frac{\partial f}{\partial r_{mn}{}^\alpha}, \tag{A2}$$

we get

$$V_{l_1\cdots l_j}{}^{\alpha_1\cdots\alpha_j}=\tfrac{1}{2}\sum_{m\neq n} v_{m-n}{}^{\alpha_1\cdots\alpha_j}\prod_{i=1}^{j}(\delta_{l_im}-\delta_{l_in}), \tag{A3}$$

where

$$v_n{}^{\alpha_1\cdots\alpha_j}=\left.\frac{\partial^j\varphi}{\partial r^{\alpha_1}\cdots\partial r^{\alpha_j}}\right|_{\mathbf{R}_n}. \tag{A4}$$

The δ products in (A3) ensure that each l belongs to one or the other of an interacting pair of atoms and give appropriate signs. The separation of l and α factors shows that the CP are now symmetric in upper and lower indices separately. The transformation relation (2.13c) implies that

$$v_{\mathcal{T}n}{}^{\alpha_1\cdots\alpha_j}=\sum_{\beta_1,\cdots,\beta_j} T_{\alpha_1\beta_1}\cdots T_{\alpha_j\beta_j}v_n{}^{\beta_1\cdots\beta_j}, \tag{A5}$$

and, in particular, that

$$v_{-n}{}^{\alpha_1\cdots\alpha_j}=(-1)^j v_n{}^{\alpha_1\cdots\alpha_j}. \tag{A6}$$

With the help of (A6) the CP with $l_j=0$, which are used in Sec. IV, can be written

$$V_{l_1\cdots l_{j-1}0}{}^{\alpha_1\cdots\alpha_{j-1}\alpha_j}=\sum_{n\neq 0} v_n{}^{\alpha_1\cdots\alpha_j}\prod_{i=1}^{j-1}(\delta_{l_i0}-\delta_{l_in}). \tag{A7}$$

The form of the derivatives (A4) for $j\leq 4$ are given in Eqs. (2.19) and (2.19a) of Ref. 8 and will not be repeated here.

The assumption of a central (Born-Mayer) potential was used here only for getting V_3 and V_4 (Sec. VII).

PHYSICAL REVIEW VOLUME 178, NUMBER 3 15 FEBRUARY 1969

Localization of Wannier Functions in Copper

D. A. GOODINGS* AND R. HARRIS†
University of Sussex, Brighton, England
(Received 16 September 1968)

The problem of constructing localized one-electron wave functions in metals having complicated band structures is considered with reference to copper. The extent to which the Wannier functions are localized depends critically on how the Bloch functions from which they are constructed are labeled with respect to the band index and on the choice of the phase factor associated with each Bloch function. A practical approach to the handling of these problems is described and calculations based on augmented-plane-wave (APW) Bloch functions for copper are reported. The resulting Wannier functions are found to be poorly localized. By relaxing the requirement of orthogonality, a set of pseudo-phase-factors can be determined so as to maximize the probability at the central site. The non-orthogonal "localized" functions which result have a definite symmetry within the central APW sphere, where they strongly resemble tight binding functions. However, their localization is generally not much better than that of the Wannier functions. The implications of our results for the Koster-Slater theory of dilute alloys and for recent developments in understanding the band structures of transition metals are briefly discussed.

1. INTRODUCTION

THE theory of impurity states in metals due to Koster and Slater[1] presents the possibility of carrying out accurate calculations of one-electron energies and wave functions. However, the success of this approach depends on the extent to which the potential of the solute atom is localized and, perhaps more crucially, on the degree of localization of the Wannier functions of the host lattice. The investigations by Kanamori[2] of iron-series alloys, by Clogston[3] of iron dissolved in 4*d*-transition metals, and by Sokoloff[4] of copper alloys rely on the assumption that the Wannier functions fall off sufficiently rapidly that matrix elements of the impurity potential connecting Wannier functions on sites separated by more than the first- or second-neighbor distance can be neglected.

The extent to which Wannier functions of transition metals are localized is also important in the work of Hubbard[5] and Kanamori[6] on the correlated motion of *d* electrons. It is assumed in their investigations that the matrix elements of the Coulomb interaction are nonzero only between Wannier functions centered on the same atom.

To our knowledge there have been few attempts to

* Present address: American University of Beirut, Beirut, Lebanon. Address after July 1969: McMaster University, Hamilton, Ontario, Canada.
† Present address: Physics Department, Imperial College, London S.W.7. England.

[1] G. F. Koster and J. C. Slater, Phys. Rev. **95**, 1167 (1954); G. F. Koster, *ibid.* **95**, 1436 (1954); G. F. Koster and J. C. Slater, *ibid.* **96**, 1208 (1954).
[2] J. Kanamori, J. Appl. Phys. **36**, 929 (1965).
[3] A. M. Clogston, Phys. Rev. **136**, A1417 (1964).
[4] J. Sokoloff, Phys. Rev. **161**, 540 (1967).
[5] J. Hubbard, Proc. Roy. Soc. (London) **A276**, 238 (1963).
[6] J. Kanamori, Progr. Theoret. Phys. (Kyoto) **30**, 275 (1963).